

PAPER • OPEN ACCESS

## Miscibility in coupled dipolar and non-dipolar Bose–Einstein condensates

To cite this article: Ramavarmaraja Kishor Kumar *et al* 2017 *J. Phys. Commun.* 1 035012

View the [article online](#) for updates and enhancements.

### Related content

- [Three-dimensional vortex structures in a rotating dipolar Bose–Einstein condensate](#)  
Ramavarmaraja Kishor Kumar, Thangarasu Sriraman, Henrique Fabrelli et al.
- [The physics of dipolar bosonic quantum gases](#)  
T Lahaye, C Menotti, L Santos et al.
- [Vortices and vortex lattices in quantum ferrofluids](#)  
A M Martin, N G Marchant, D H J O'Dell et al.



## PAPER

## Miscibility in coupled dipolar and non-dipolar Bose–Einstein condensates

## OPEN ACCESS

## RECEIVED

12 June 2017

## REVISED

5 September 2017

## ACCEPTED FOR PUBLICATION

19 September 2017

## PUBLISHED

1 November 2017

Original content from this work may be used under the terms of the [Creative Commons Attribution 3.0 licence](#).

Any further distribution of this work must maintain attribution to the author(s) and the title of the work, journal citation and DOI.

Ramavarmaraja Kishor Kumar<sup>1</sup>, Paulsamy Muruganandam<sup>1,2</sup> , Lauro Tomio<sup>3,4</sup>  and Arnaldo Gammal<sup>1</sup><sup>1</sup> Instituto de Física, Universidade de São Paulo, 05508-090 São Paulo, Brazil<sup>2</sup> Department of Physics, Bharathidasan University, Tiruchirappalli 620024, India<sup>3</sup> Instituto de Física Teórica, UNESP, 01156-970 São Paulo, Brazil<sup>4</sup> Instituto Tecnológico de Aeronáutica, DCTA, 12.228-900 S. J. dos Campos, BrazilE-mail: [tomio@ift.unesp.br](mailto:tomio@ift.unesp.br)**Keywords:** ultracold trapped gases, multicomponent dipolar condensates, miscibility, matter wavers**Abstract**

We perform a full three-dimensional study on miscible-immiscible conditions for coupled dipolar and non-dipolar Bose–Einstein condensates (BEC), confined in anisotropic traps. In view of recent experimental studies, our focus was the atomic erbium–dysprosium (<sup>168</sup>Er–<sup>164</sup>Dy) and dysprosium–dysprosium (<sup>164</sup>Dy–<sup>162</sup>Dy) mixtures. The miscibility is quantified by the overlap of the two-component densities, using an appropriate defined parameter. By verifying that stable regimes for pure-dipolar coupled BECs are only possible in pancake-type traps, we obtain some non-trivial local minimum biconcave-shaped states with density oscillations in both components. For non-dipolar systems with repulsive interactions, we show that immiscible stable configurations are also possible in cigar-type geometries. The main role of the trap aspect ratio and inter-species contact interaction for the miscibility is verified for different configurations, from non-dipolar to pure dipolar systems.

**1. Introduction**

Following the first experimental realization of Bose–Einstein condensation (BEC) in 1995 [1], substantial progress has been verified in experimental and theoretical investigations with ultracold quantum gases, which can be traced by several paper reviews on the subject (as references in [2]), as well as by a recent book written by experts in the field [3]. One can also follow the advances in quantum simulations and control of BECs in reviews such as [4, 5]. From studies with ultra-cold atoms, we can improve our understanding on quantum properties of a large variety of bosonic and fermionic systems, as well as molecular configurations with different atomic species. By controlling atomic properties potential technological applications exist from ultra-precise clocks till quantum computation. In this respect, by considering BEC mixing with different atomic and molecular configurations, also with degenerate complex atoms (alkaline-earth, lanthanides) and Fermi gases, one can investigate the crossover of BEC properties with Bardeen–Cooper–Schrieffer superconductivity, superfluid to Mott insulator transition in bosonic and fermionic systems, quantum phases of matter in optical lattices, ground-state fermionic molecules [6].

BEC with two-components was first produced with different hyperfine states of <sup>87</sup>Rb [7]. This is a simple example of a multicomponent system made with a mixture of two-species of bosons. Following that, one should notice several investigations using binary mixtures. This can be exemplified with works considering the dynamics of binary mixtures with bosons and fermions [8]; studies on the dynamics of phase separation and on how to control it [9, 10]; also considering mixtures with different isotopes of the same atomic species [11], or with different atomic species [12]. As a relevant characteristics of multicomponent ultracold gases, we have their miscibility behavior which will depend on the nature of the interatomic interactions between different species. Miscible or immiscible two-component BEC systems can be distinguished by the spatial overlap or separation of the respective wave-functions of each component. Their phase separations were observed in spinor BECs of sodium in all hyperfine states of  $F = 1$  [13]. The advances in the experimental investigations with multi-component BECs have

activated a large amount of theoretical descriptions applied to condensed mixtures having spatially segregated phases, by studying their properties related to static and dynamical stability [14–26].

Dipolar atomic and molecular systems, as well as mixtures with different dipolar atoms, have been explored in theoretical works connected with BEC since 2000 [27, 28], followed by several other investigations motivated by the increasing experimental possibilities in cold-atom laboratories to probe the theoretical analysis and eventual proposals. The theoretical effort in this direction can be traced back by the following sample works, [29–41]. A more complete bibliography on the subject, covering experimental and theoretical approaches, can be found in recent reviews and dissertations, as given in [41–45].

When considering the investigations with dipolar systems in cold-atom laboratories, the pioneer work is the experiment with chromium  $^{52}\text{Cr}$ , reported in [46]. Among the works following that, we have the investigations on the stability of dipolar gases [34], as well as on collisions of dipolar molecules [47]. With ultra-cold atoms having non-negligible magnetic moments, we have experiments with dysprosium described in [48], considering the dysprosium isotopes  $^{162,164}\text{Dy}$ ; and the investigation with erbium  $^{168}\text{Er}$  in [42]. More recently, quantum droplets have been observed in a strongly dipolar condensed gas of  $^{164}\text{Dy}$  [49], with new features being verified for dipolar BECs, due to the competition between isotropic short-range contact interaction and anisotropic long-range dipole–dipole interaction (DDI).

By considering the quite interesting recent investigations in ultracold laboratories with two-component dipolar BECs, studies on stability and miscibility properties are of interest due to the number of control parameters that can be explored in new experimental setups. The parameters are given by the strength of dipoles, number of atoms in each component, inter- and intra-species scattering lengths, as well as confining trap geometries or optical lattices. Among the theoretical studies cited above (most concentrated on stability of dipolar condensates), we have some of them are particularly related to miscibility of coupled BECs and structure formation, as [19, 31, 37, 40].

In the present paper, our main proposal is to discuss miscibility conditions for general three-dimensional (3D) atomic BEC systems, which are constituted by two-coupled dipolar or non-dipolar species confined by asymmetric cylindrical harmonic traps. Due to stability requirements, the dipolar systems that we are considering will be confined in pancake-type traps. In case of non-dipolar coupled systems, we also discuss the miscibility by considering cigar-type symmetries. For our study on the miscibility, we start with a brief discussion by considering the homogeneous case. In order to simplify the formalism and a possible experimental realization, both species are assumed to be confined by a cylindrical trap with the same aspect ratio. Without losing the general conclusions related to miscibility of two-atomic dipolar BEC species, most of our study will focus on the particular  $^{168}\text{Er}$ – $^{164}\text{Dy}$  and  $^{164}\text{Dy}$ – $^{162}\text{Dy}$  mixtures, motivated by the actual experimental possibilities [42, 48].

Our numerical results for the coupled dipolar Gross–Pitaevskii (GP) equation are presented by using different parameter configurations for the trapping properties, as well as for the inter- and intra-species two-body contact and dipolar interactions. The parameter region of stability for the dipolar system is discussed for different trap-aspect ratio and number of atoms in each species. As we are going to evidence, for a given mixture of two condensates confined by harmonic traps, the main parameters of the system that are possible to be manageable in an experimental realization with focus on the miscibility are the trap-aspect ratio and the two-body scattering lengths (these ones, controlled via Feshbach resonance techniques [5, 50]).

Within our full-3D model for the coupled densities, when considering pure dipolar systems trapped in pancake-shaped harmonic potentials, we are also discussing some unusual local minimum structures and fluctuations in the densities, which are verified when the system is near the instability border (considering the critical aspect ratio and atom numbers). These structures are verified for coupled systems that are partially immiscible ( $^{168}\text{Er}$ – $^{164}\text{Dy}$ , in the present case), as well as when it is completely miscible, such as  $^{164}\text{Dy}$ – $^{162}\text{Dy}$ . Such structures, verified for well defined trap-aspect ratio and number of atoms in stable configurations, suggest possible experimental studies with two-component dipolar BECs, considering miscible and immiscible systems.

The next sections are organized as follows. In section 2, we present the general 3D mean-field formalism (in full-dimension and dimensionless) for trapped two-component dipolar BECs, together with the definition of relevant parameters, as well as the numerical approach we are considering. In section 3, we first write down the miscibility conditions for homogeneous coupled systems, followed by the definition of an appropriate miscibility parameter, which is found appropriate to measure the overlap between densities of a general coupled system. Our numerical results are organized in two sections, in order to characterize the main relevant conditions for the observation of miscibility in coupled BEC systems. The role of the trap symmetry for the miscibility, considering different dipolar and non-dipolar mixed systems, is analyzed in section 4. In view of the particular relevance of the inter-species two-body interactions on the miscibility, the corresponding results are presented and discussed in section 5. Finally, in section 6, we present a summary with our principal conclusions and perspectives.

## 2. Formalism for coupled BEC with dipolar interactions

For a mixed system with two atomic species identified by  $i = 1, 2$ , having their masses, number of particles and local time-dependent wave-functions given by  $m_i, N_i$  and  $\psi_i \equiv \psi_i(\mathbf{r}, t)$ , respectively, the general form of the mean-field GP equation, for the trapped system with dipolar interactions, can be described by [29],

$$i\hbar \frac{\partial \psi_i(\mathbf{r}, t)}{\partial t} = \left[ -\frac{\hbar^2}{2m_i} \nabla^2 + V_i(\mathbf{r}) + \sum_{j=1}^2 G_{ij} N_j |\psi_j(\mathbf{r}, t)|^2 + \sum_{j=1}^2 \frac{N_j}{4\pi} \int d^3\mathbf{r}' V_{ij}^{(d)}(\mathbf{r} - \mathbf{r}') |\psi_j(\mathbf{r}', t)|^2 \right] \psi_i(\mathbf{r}, t), \quad (1)$$

where  $V_i(\mathbf{r})$  is the trap potential for each species  $i$ , with  $V_{ij}^{(d)}(\mathbf{r} - \mathbf{r}')$  defining the magnetic-type dipolar interaction between particles  $i$  and  $j$ . The nonlinear contact interactions between the particles are given by  $G_{ij} \equiv (2\pi\hbar^2/m_{ij})a_{ij}$ , where  $a_{11}, a_{22}$  and  $a_{12} = a_{21}$  are the two-body scattering lengths for intra ( $a_{ii}$ ) and inter ( $a_{12}$ ) species, with  $m_{ij}$  being the reduced mass  $m_i m_j / (m_i + m_j)$ . In the above, both wave-function components are normalized as

$$\int d^3\mathbf{r} |\psi_i(\mathbf{r}, t)|^2 = 1. \quad (2)$$

For the confining trap potentials we assume harmonic cylindrical shapes, with frequencies  $\omega_i$  and aspect ratios  $\lambda_i$ , such that

$$V_i(\mathbf{r}) = \frac{m_i \omega_i^2}{2} (r_1^2 + r_2^2 + \lambda_i^2 r_3^2), \quad (3)$$

where it will be assumed that each species  $i$  is confined by an angular frequency  $\omega_i$  along the  $x$ - $y$  plane,  $\vec{\rho} \equiv r_1 \hat{e}_1 + r_2 \hat{e}_2$ ; and with  $\lambda_i \omega_i$  along the  $z$ -direction  $r_3 \hat{e}_3$ . The trap will be spherically symmetric for  $\lambda_i = 1$ ; will have a cigar shape for  $\lambda_i < 1$ ; and a pancake shape when  $\lambda_i > 1$ .

For the magnetic-type dipolar interaction between particles  $i$  and  $j$ , with respective dipole momentum strength given by  $D_{ij} \equiv \mu_0 \mu_i \mu_j$  ( $\mu_0$  being the permeability in free space and  $\mu_i$  the dipole moment of the species  $i$ ), we have

$$V_{ij}^{(d)}(\mathbf{r} - \mathbf{r}') = D_{ij} \frac{1 - 3 \cos^2 \theta}{|\mathbf{r} - \mathbf{r}'|^3}, \quad (4)$$

where  $\mathbf{r} - \mathbf{r}'$  determines the relative position of dipoles and  $\theta$  is the angle between  $\mathbf{r} - \mathbf{r}'$  and the direction of polarization.

Let us rewrite (1) in dimensionless quantities, with the first component defining the scales for length, with  $l \equiv \sqrt{\hbar / (m_1 \omega_1)}$  and energy,  $\hbar \omega_1$ . Within these units, we introduce new dimensionless variables and redefine the parameters such that

$$\begin{aligned} \mathbf{x} &\equiv \frac{\mathbf{r}}{l} = x \hat{e}_1 + y \hat{e}_2 + z \hat{e}_3 \equiv \vec{\rho} + z \hat{e}_3; \quad \nabla_{\mathbf{x}} = l \nabla_{\mathbf{r}}, \quad \tau \equiv \omega_1 t, \\ g_{ij} &\equiv \frac{G_{ij} N_j}{\hbar \omega_1 l^3} = \frac{2\pi m_1 a_{ij} N_j}{m_{ij} l}, \quad \sigma \equiv \frac{m_2 \omega_2^2}{m_1 \omega_1^2}, \\ a_{ii}^{(d)} &= \frac{D_{ii}}{12\pi} \frac{m_i}{m_1} \frac{1}{\hbar \omega_1 l^2}, \quad a_{12}^{(d)} = a_{21}^{(d)} = \frac{D_{12}}{12\pi} \frac{1}{\hbar \omega_1 l^2}, \\ d_{ij} &= \frac{N_j D_{ij}}{4\pi} \frac{1}{\hbar \omega_1 l^3}. \end{aligned} \quad (5)$$

With the above, and also by redefining the wave-functions for the atomic species  $i$ ,  $\phi_i(\mathbf{x}, \tau) = \sqrt{l^3} \psi_i(\mathbf{r}, t)$ , the expression (1) can be rewritten as the following dimensionless coupled expressions:

$$i \frac{\partial \phi_1}{\partial \tau} = \left[ -\frac{1}{2} \nabla_{\mathbf{x}}^2 + \frac{1}{2} (\rho^2 + \lambda_1^2 z^2) + g_{11} |\phi_1|^2 + g_{12} |\phi_2|^2 + \int d^3\mathbf{y} \frac{1 - 3 \cos^2 \theta}{|\mathbf{x} - \mathbf{y}|^3} (d_{11} |\phi_1|^2 + d_{12} |\phi_2|^2) \right] \phi_1 \quad (6)$$

and

$$i\frac{\partial\phi_2}{\partial\tau} = \left[ -\frac{m_1}{2m_2}\nabla_x^2 + \frac{\sigma}{2}(\rho^2 + \lambda_2^2 z^2) + g_{21}|\phi_1|^2 + g_{22}|\phi_2|^2 + \int d^3y \frac{1 - 3\cos^2\theta}{|\mathbf{x} - \mathbf{y}|^3} (d_{21}|\phi_1'|^2 + d_{22}|\phi_2'|^2) \right] \phi_2, \quad (7)$$

where  $\phi_i \equiv \phi_i(\mathbf{x}, \tau)$  and  $\phi_i' \equiv \phi_i(\mathbf{y}, \tau)$ .

### 2.1. Dipolar and contact interaction parameters

In our analysis, two kind of coupled atomic system are being treated. First, with the erbium  $^{168}\text{Er}$  and dysprosium  $^{164}\text{Dy}$ , assumed with moment dipoles  $\mu = 7\mu_B$  and  $\mu = 10\mu_B$ , respectively ( $\mu_B$  is the Bohr magneton). Next, both components of the coupled system are from isotopes of the same atomic species,  $^{164}\text{Dy}$  and  $^{162}\text{Dy}$ , such that the moment dipoles are the same  $\mu = 10\mu_B$  for both components. As a rule we define as component 1 in the mixture the more massive atomic species.

For the angular frequencies of the axial traps, we use  $\omega_1 = 2\pi \times 60 \text{ s}^{-1}$  for the  $^{168}\text{Er}$  and  $\omega_2 = 2\pi \times 61 \text{ s}^{-1}$  for  $^{164}\text{Dy}$  and  $^{162}\text{Dy}$ , corresponding to  $\sigma \approx 1$ , with equal aspect ratios for both components:  $\lambda \equiv \lambda_1 = \lambda_2$ . The time and space units will be such that  $\omega_1^{-1} = 2.65 \text{ ms}$  and  $l = 1\mu\text{m}$  ( $=10^4 \text{ \AA} = 1.89 \times 10^4 a_0$ ). In case of purely dipolar BECs, we take all the two-body scattering lengths  $a_{ij} = 0$ . In several other cases we fix the scattering lengths between  $10a_0$  and  $110a_0$ , where  $a_0$  is the Bohr radius. In order to compare the dipolar and contact interactions, the parameters for the intra- and inter-species dipolar interactions are given in terms of the length scale. For the moment dipole of the species, in terms of the Bohr magneton  $\mu_B$ , we assume  $\mu = 7\mu_B$  for  $^{168}\text{Er}$ , with  $\mu = 10\mu_B$  for both species of dysprosium,  $^{164,162}\text{Dy}$ . The two-body scattering lengths  $a_{ij}$  and dipolar interactions  $a_{ij}^{(d)}$ , given in units of  $a_0$ , are related to the corresponding dimensionless parameters  $g_{ij}$  and  $d_{ij}$  as:  $a_{11}/a_0 \approx 1504g_{11}/N_1$ ,  $a_{ij \neq 11}/a_0 \approx 1486g_{ij}/N_j$ ,  $a_{11}^{(d)}/a_0 \approx 6301d_{11}/N_1$ ,  $a_{22}^{(d)}/a_0 \approx 6151d_{22}/N_2$ ,  $a_{12}^{(d)}/a_0 \approx 6301d_{21}/N_1 = 6301d_{12}/N_2$ .

### 2.2. Numerical approach

For the numerical approach, used to obtain our results when solving the full-3D coupled equations (6) and (7), we have employed the split-step Crank–Nicolson method, which is detailed in similar nonlinear studies, as in [17, 51], where one can find more extended analysis and details on computer techniques convenient for nonlinear coupled equations, facing stability and accuracy of the results. In view of the particular integro-differential structure of the coupled nonlinear differential equations when having dipolar interactions, we had to combine our approach in solving coupled differential equations with a standard method for evaluating dipolar integrals in momentum space [29, 52, 53].

By looking for stable solutions, the 3D numerical simulations were carried out in imaginary time with a grid size having 128 points for each dimension, where we have  $\Delta x = \Delta y = \Delta z = 0.2$  for the space-steps and  $\Delta t = 0.004$  for the time-step. The results were quite stable, verified by taking half of the mentioned grid sizes.

As a preliminary calculation, which also help us to check the numerical code, we reproduce the stability diagram obtained in [29] for a spherically symmetric trap ( $\lambda = 1$ ), where only one atomic species was used,  $^{52}\text{Cr}$ , for the coupled system, with the two species ( $m_1 = m_2$ ) having opposite polarizations along the  $z$  direction. Besides that, in our analysis, we have also verified the stability of the numerical results by studying the effect of varying  $\lambda$ . In this regard, once verified that pancake-type configurations are required for stable dipolar configurations, the miscibility in cigar-type traps is being analyzed only for non-dipolar systems.

## 3. Miscibility of coupled systems

### 3.1. Homogeneous case with hard-wall barriers

In order to characterize the transition between miscible and immiscible states, let us consider a simpler case, for the homogeneous 3D system with  $V_1(\mathbf{r}) = V_2(\mathbf{r}) = 0$  and hard-wall barriers, following the simplified energetic approach presented in [15]. Within this approximation, the miscible-immiscible transition (MIT) can be characterized by a threshold parameter, which is defined by the relation between the two-body repulsive interactions. The criterium for miscibility, also quoted in some recent works on binary BEC mixtures (see, for instance, [19, 21]), was previously obtained from stability analysis of the excitation spectrum in [14]. It can be easily generalized to include all the two-body repulsive interactions.

As in the present case we are interested in mixed configuration with contact and dipolar interactions, we should first obtain a simple relation for the dipolar interactions appearing in the formalism. For that, we follow the approach given in [29] to deal with the integro-differential formalism where we have a divergence of the

integrand in the zero limit for the inter-particle distances. The convolution theorem and Fourier transforms are applied for the magnetic dipolar potential and for the density components  $|\psi_i|^2$ . The Fourier transform of the dipolar potential (4) is given in terms of a cut-off parameter, which is of the order of the atomic radius. As this parameter is much smaller than a significant length scale of the system, one can safely consider the limit where it is zero, such that the dipolar potential between the atomic species  $i$  and  $j$  is given by

$$\mathcal{V}_{ij}^{(d)}(\mathbf{k}) = D_{ij} \frac{4\pi}{3} (3 \cos^2 \theta_{\mathbf{k}} - 1) \equiv D_{ij} \frac{4\pi}{3} f(\theta_{\mathbf{k}}), \quad (8)$$

where  $\theta_{\mathbf{k}}$  is the angle between the wave-vector  $\mathbf{k}$  and the dipole moment.

Therefore, by including together the contact and dipolar interactions, the condition for MIT can be written as

$$\Delta = \frac{|G_{11} + D_{11}f(\theta_{\mathbf{k}})||G_{22} + D_{22}f(\theta_{\mathbf{k}})|}{[G_{12} + D_{12}f(\theta_{\mathbf{k}})]^2} - 1, \quad (9)$$

where  $\Delta = 0$  defines the critical value for the transition from miscible ( $\Delta > 0$ ) to immiscible ( $\Delta < 0$ ) systems. The mixed coupled state will have a lower total energy when the mutual repulsion between atoms is large enough such that we have  $\Delta < 0$ , which is characterizing the system in an immiscible phase. The system will be in a miscible phase when  $\Delta > 0$ , with a critical border for the transition given by  $\Delta = 0$ . The MIT occurs when the inter-species and intra-species interactions are balanced. As verified, the two-body interactions are just being scaled by the dipolar interactions, in this simple case that the system is confined by hard-wall barriers. The observation that the dipolar interactions are not playing a significant role results from the fact that the DDIs averaged out for homogeneous gases. However, for numerical comparisons with more general miscibility conditions, it is still quite useful, as it does not depend on the number of atoms and condensate size.

### 3.2. Miscibility in general coupled systems

The miscible to immiscible transition for a coupled system, as defined by the critical limit  $\Delta$  in (9), is changed from a first-order transition that occurs for homogeneous system to a second-order one when the kinetic energy is taken into account, as discussed in [20]. Therefore, in order to evaluate the miscibility of a coupled system for a more general case, we define a parameter which gives an approximate measure of how much overlapping we have between the densities of both components. By the definition of a parameter related to the densities we are modifying the one suggested in [20], where the overlap between the wave-functions was considered. Both definitions are equivalent in particular cases. Our parameter to define the miscibility of a coupled system is given by

$$\eta = \int |\phi_1||\phi_2| \, dx = \int \sqrt{|\phi_1|^2|\phi_2|^2} \, dx. \quad (10)$$

As  $\phi_1$  and  $\phi_2$  are both normalized to one, also having the same center, this expression implies that  $\eta = 1$  for the complete overlap between the two densities, decreasing as the overlap diminishes. Therefore, we can define the system as almost completely immiscible when  $\eta \ll 1$  (close to zero); and, almost completely miscible when  $\eta$  is close to one. This parameter is extending to general non-homogeneous mixtures the MIT criterium (9) discussed for homogeneous systems. With  $\eta$ , intermediate cases can be determined when the system is partially immiscible or partially miscible. From our observation, which will follow from the analysis of results obtained for the densities in the next sections, when  $\eta \lesssim 0.5$  the system shows already a clear space separation, with the components having their maxima in well separated points in the space, such that we can already define the coupled system as immiscible. For  $\eta$  between 0.5 and 0.8, the two densities start having an increasing overlap with their maxima approaching each other, such that we can define the system within this interval as partially miscible. The maxima of the densities are close together for  $\eta \gtrsim 0.8$ , when we assume the system is miscible.

As a side remark, we should observe that we are treating two condensates with different atomic species symmetrically distributed around the center. As a general expected behavior, the density of the more massive species should be closer to the center, with the other density being pushed out. This can be explained even before activating particular interactions between the atoms, as the kinetic energy of the massive species is smaller than the corresponding kinetic energy of the less massive species.

Next two sections are dedicated to present our main results on the miscibility of coupled dipolar and non-dipolar BECs. When choosing non-zero dipolar parameters, the results are exemplified by two mixtures for a better characterization of the miscibility properties. Within the actual experimental possibilities in BEC laboratories, we consider the erbium–dysprosium ( $^{168}\text{Er}$ – $^{164}\text{Dy}$ ) and dysprosium–dysprosium ( $^{164}\text{Dy}$ – $^{162}\text{Dy}$ ) mixtures.

## 4. Miscibility results—role of the trap symmetry

The results analyzed in this section for the miscibility properties of coupled atomic condensates are more concerned with the role of the symmetry of the harmonic trap, considering different configurations for the possible internal interactions (contact and dipolar) between the atoms of both species. The contact interactions are characterized by the atomic two-body scattering lengths, with dipolar interactions due to the magnetic dipole moment of each atomic species. In the following, we split the section in three subsections for clarity. In part A, we consider miscibility in the case we have no contact interactions, starting with a discussion on the stability of such dipolar systems in terms of the trap-aspect ratio and number of atoms. As shown, for realistic number of atoms, we need pancake-shaped traps. Next, in part B, our analysis is concentrated in non-dipolar coupled structures, where we can examine cigar-type and pancake-type BEC configurations. We conclude the section with part C, by analyzing our results for the case that we have both dipolar and contact interactions.

### 4.1. Miscibility in pure dipolar interactions

#### 4.1.1. Stability analysis

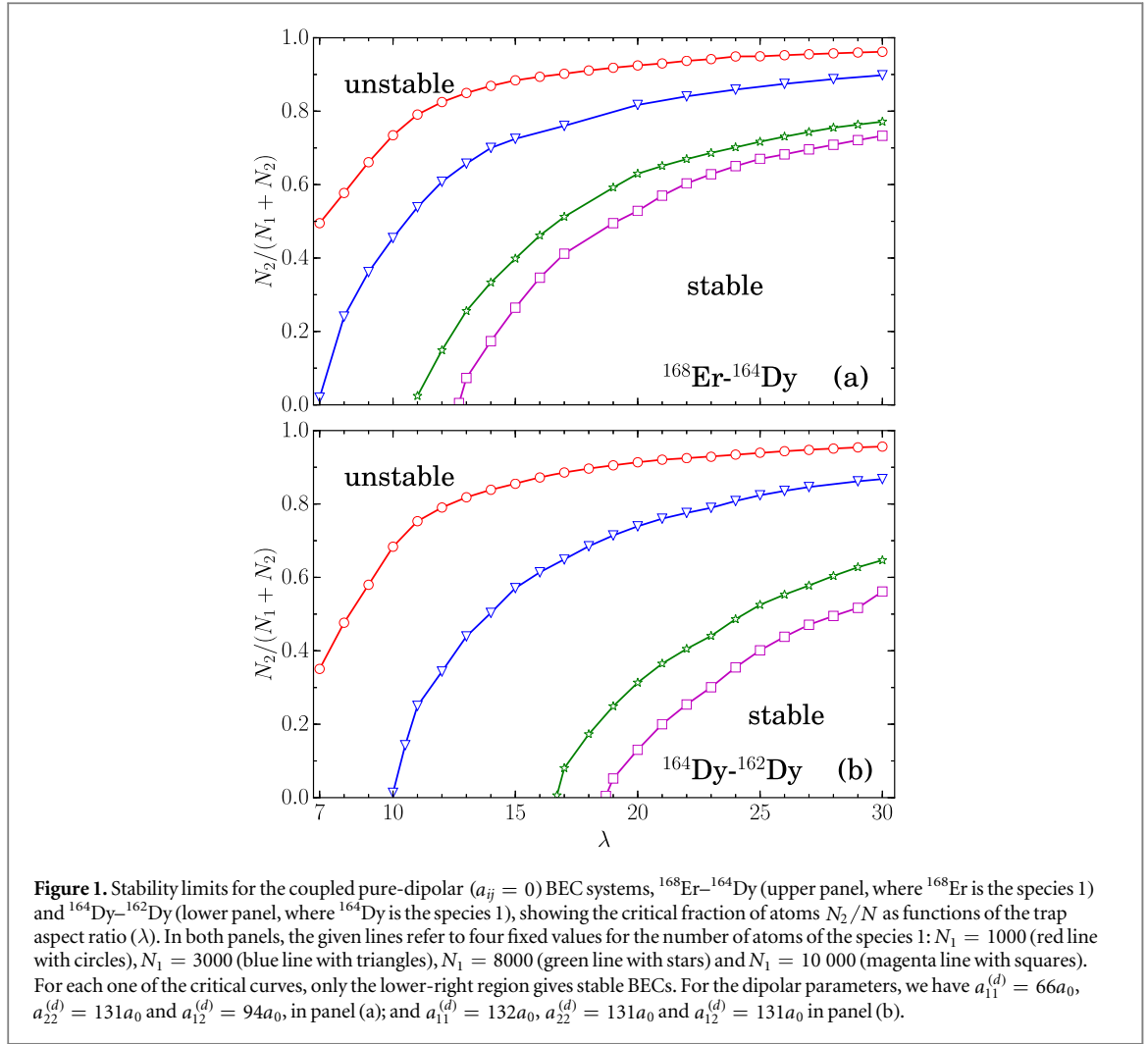
The homogeneous case of purely dipolar condensate is unstable due to anisotropy of the DDI. However, in a way similar as the case of homogeneous non-dipolar BEC that are unstable (for attractive two-body interactions,  $a < 0$ ), the instability usually can be overcome by applying some external trap, which will help to stabilize the dipolar BEC by imprinting anisotropy to the density distribution [34]. This is applicable for single and multi-component dipolar BECs. On the stability of two condensates purely dipolar, separated by a distance, we can mention [38]. For the case of single component dipolar condensates, it was previously shown in [27, 28] that, by increasing the aspect ratio  $\lambda$  one can obtain a more stable configuration due to the DDI becoming effectively more repulsive.

As shown by the stability diagrams given in the two panels of figure 1, pure dipolar condensates require pancake-type traps to be stable, with the coupled mixture becoming less stable when the dipolar strengths (inter and intra-species) are close to the same values (for some fixed ratio of number of atoms in both species). This effect is mainly due to the inter-species repulsion in comparison with the corresponding intra-species ones.

To become clear this effect, our results are given for the coupled equations (6) and (7), considering the dipolar BEC mixtures with  $^{168}\text{Er}$ – $^{164}\text{Dy}$  (upper panel), where  $^{168}\text{Er}$  (1st component) and  $^{164}\text{Dy}$  (2nd component) and  $^{164}\text{Dy}$ – $^{162}\text{Dy}$  (lower panel), where  $^{164}\text{Dy}$  (1st component) and  $^{162}\text{Dy}$  (2nd component). The fraction number of atoms  $N_2/N$ , where  $N \equiv (N_1 + N_2)$  is shown as a function of the aspect ratio  $\lambda$ , considering four sample fixed values for the component 1 of the mixture, which are given by  $N_1 = 1000$  (red lines with circles), 3000 (blue lines with triangles), 8000 (green lines with stars) and 10 000 (magenta lines with squares). In both the cases, we use purely dipolar BECs ( $a_{ij} = 0$ ). The dipolar parameters of the  $^{168}\text{Er}$ – $^{164}\text{Dy}$  coupled system are  $a_{11}^{(d)} = 66a_0$ ,  $a_{22}^{(d)} = 131a_0$  and  $a_{12}^{(d)} = 94a_0$ . Also, the dipolar parameters of the  $^{164}\text{Dy}$ – $^{162}\text{Dy}$  mixtures are  $a_{11}^{(d)} = 132a_0$ ,  $a_{22}^{(d)} = 131a_0$  and  $a_{12}^{(d)} = 131a_0$ . From both the panels, one can extract the information that the stability of pure-dipolar mixtures is mainly affected by the inter-species strengths of the dipolar interactions (in comparison with the corresponding intra-species strengths). The systems are more stable if less repulsion occurs between inter-species atoms. By comparing the lower with the upper panel, we can verify the effect of reducing by about half the dipolar strength of one of the component, increasing the stability of the system. The maximum effect can be seen for  $N_2 = 0$  ( $N = N_1$ ), implying that a system with 10 000 atoms of  $^{168}\text{Er}$  can only be stable within a pancake-like trap with  $\lambda \gtrsim 13$ , whereas with the same number of  $^{164}\text{Dy}$  atoms the stability can only be reached for  $\lambda \gtrsim 19$ .

For a fixed aspect ratio  $\lambda$ , the two-component BEC can become unstable by increasing the fraction  $N_2/N$ , where the critical number varies according to the fraction  $N_1/N$ . Also, there is a critical trap aspect ratio ( $\lambda_c$ ) for the stability, As one can verify from the upper panel, for the  $^{168}\text{Er}$ – $^{164}\text{Dy}$  mixture with  $N_1 = 3000, 8000$ , and 10 000 the, this critical aspect ratio starts from  $\lambda_c \approx 7, 11$ , and 13 respectively. On the other case, for the  $^{164}\text{Dy}$ – $^{162}\text{Dy}$  mixture with the same sets of  $N_1$  ( $= 3000, 8000$ , and 10 000), the critical lower limit for stability starts with  $\lambda_c \approx 10, 17$ , and 19 respectively. This variation in the  $\lambda_c$  is obviously explained by the difference in the dipolar strengths of both the cases, with the  $^{168}\text{Er}$  component having about half of the dipolar strength of  $^{162,164}\text{Dy}$ .

From the upper panel in figure 1, for the same total number of atoms of  $^{168}\text{Er}$ – $^{164}\text{Dy}$  mixture, one can verify that, for stability,  $\lambda_c$  is reduced (less deformed pancake-type trap) when considering  $N_1 > N_2$ ; implying larger fraction of  $^{168}\text{Er}$  atoms. As an example, for  $(N_1, N_2) = (3000, 8000)$  we have  $\lambda_c \approx 16$ ; and for  $(N_1, N_2) = (8000, 3000)$  we have  $\lambda_c \approx 14$ . This behavior results from the respective strengths of the dipolar interactions of both components, with the erbium component having  $a_{11}^{(d)} = 66a_0$ , which is smaller than the corresponding value for the dysprosium component ( $a_{22}^{(d)} = 131a_0$ ). For the other case shown in the lower panel



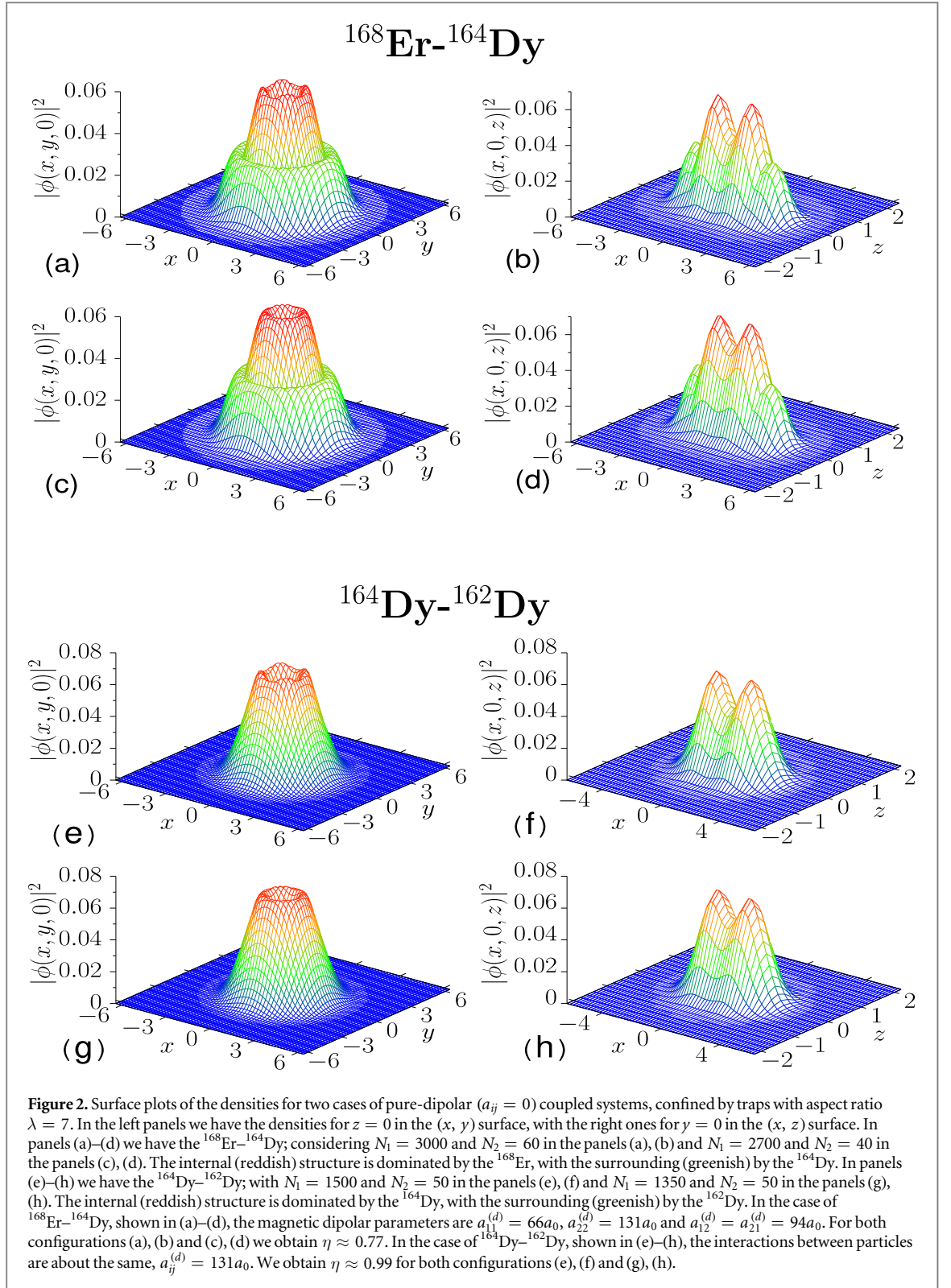
of figure 1, as both components have about equal DDI strengths,  $\lambda_c$  depends essentially only on the total number of atoms.

This stability analysis will be considered in the following study on the miscibility of two coupled mixtures. However, it can also be of interest for corresponding experimental investigations (for the specific mixtures we have considered or for other similar dipolar mixtures).

#### 4.1.2. Structure of coupled pure-dipolar condensates

Once analyzed the stability for pure dipolar coupled systems, in this subsection we characterize the role of the trapping aspect ratio  $\lambda$  in the structure and miscibility of a pure-dipolar coupled condensate. Therefore, as in the preceding subsection, all the two-body scattering lengths ( $a_{ij} = 0$ ) are fixed to zero and we consider both coupled systems with  $^{168}\text{Er}$ - $^{164}\text{Dy}$  and  $^{164}\text{Dy}$ - $^{162}\text{Dy}$ . Our numerical results for the structure of the coupled system can be visualized through density plots, with the immiscible and miscible regimes characterized by the parameter  $\eta$  defined by (10). In figure 2 we present 3D surface plots for the densities  $|\phi(x, y, 0)|^2$  in the (frames (a), (c), (e), (g)) and  $|\phi(x, 0, z)|^2$  (frames (b), (d), (f), (h)), given respectively in the  $(x, y)$  and  $(x, z)$  surfaces. These plots are providing a 3D visualization of the density overlapping and distribution of the two-components. More close to the center, we have the more massive component (in red) of the mixture, which is enhanced when the system is more immiscible. How close to the center is the other species (in green) will depend on how miscible is the mixture, being clearly identified for immiscible mixtures. This can be verified by comparing the set of panels (a)–(d) for  $^{168}\text{Er}$ - $^{164}\text{Dy}$  with the ones (e)–(h) for  $^{164}\text{Dy}$ - $^{162}\text{Dy}$ .

Corresponding to the panels of figure 2, we also have the one-dimensional (1D) plots for the densities in figure 3, which are given as functions of one of the dimensions,  $x$  or  $z$ , with the other two dimensions at the center. From these 1D densities, the amount of overlapping between the densities can better be observed, being more helpful when comparing different parameter configurations. Both systems,  $^{168}\text{Er}$ - $^{164}\text{Dy}$  and  $^{164}\text{Dy}$ - $^{162}\text{Dy}$ , represented in figures 2 and 3, are been shown for pancake-shaped traps with  $\lambda = 7$ . The number of atoms that was considered was dictated by the stability of the mixtures (as one can follow from figure 1), such that we can



study the density properties when the mixtures are stable but not far from the border where they can become unstable.

In figure 2, panels (a)–(d), for the  $^{168}\text{Er}-^{164}\text{Dy}$  mixture we use two different set of parameters for the dipolar interactions, such that we have the same value for the miscibility parameter ( $\eta = 0.77$ ). In the upper frames (a), (b) we have  $d_{11} = 31.42$ ,  $d_{12} = 0.89$ ,  $d_{22} = 1.278$  and  $d_{21} = 44.76$ , with  $N_1 = 3000$  and  $N_2 = 60$ ; in the lower frames (c), (d),  $d_{11} = 28.2$ ,  $d_{12} = 0.59$ ,  $d_{22} = 0.85$  and  $d_{21} = 40.2$ , with  $N_1 = 2700$  and  $N_2 = 40$ . The same densities are shown in 1D plots, in the four panels (a)–(d) of figure 3, in correspondence with the panels (a)–(d) of figure 2, to improve the visualization of the overlap between densities. Both components of the densities are given as functions of  $x$  (left panels) and  $z$  (right panels), with the other dimensions at the center. Note that the

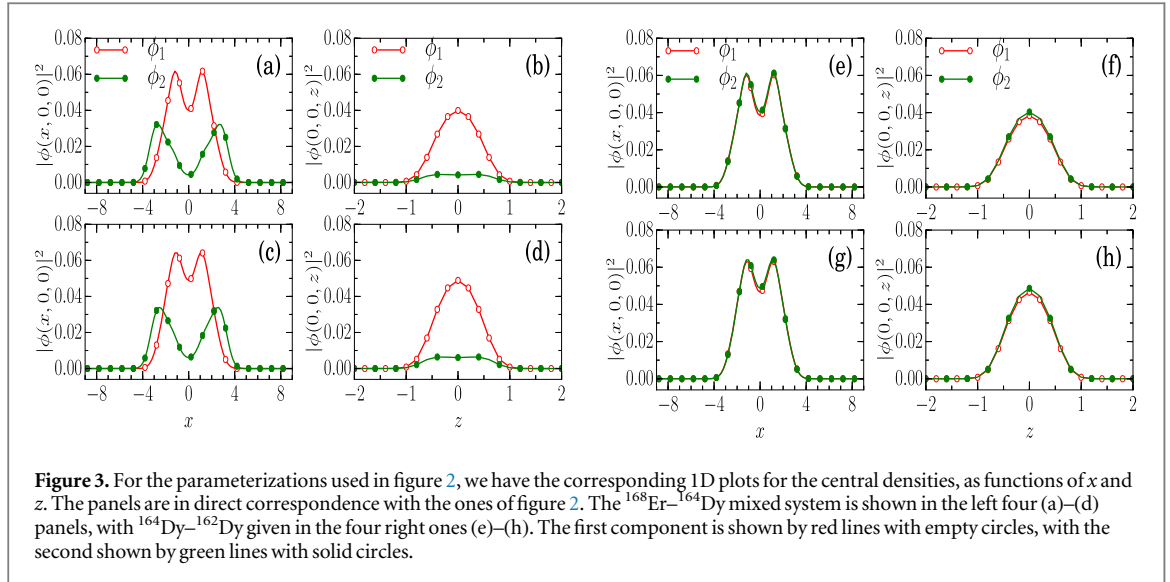


**Figure 3.** For the parameterizations used in figure 2, we have the corresponding 1D plots for the central densities, as functions of  $x$  and  $z$ . The panels are in direct correspondence with the ones of figure 2. The  $^{168}\text{Er}$ – $^{164}\text{Dy}$  mixed system is shown in the left four (a)–(d) panels, with  $^{164}\text{Dy}$ – $^{162}\text{Dy}$  given in the four right ones (e)–(h). The first component is shown by red lines with empty circles, with the second shown by green lines with solid circles.

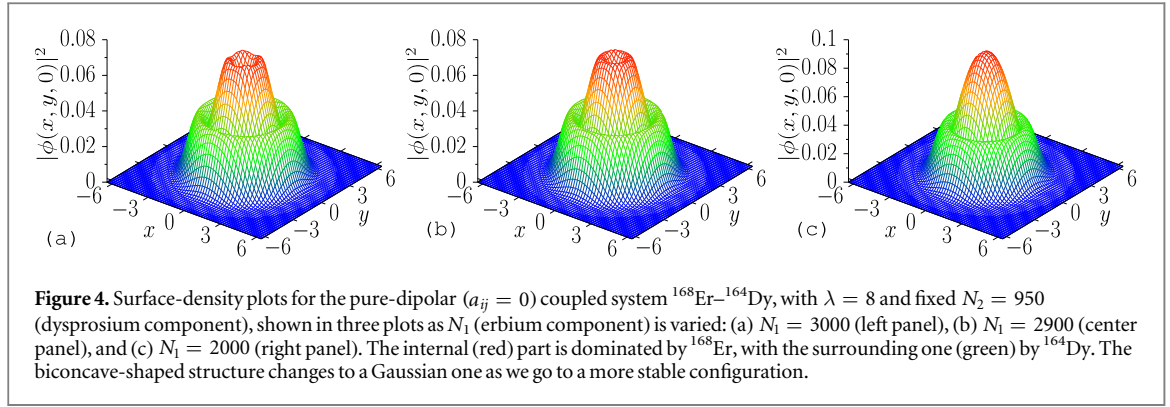
condensate is confined in a pancake-type cylindrical trap, with aspect ratio  $\lambda = 7$ , such that the distribution along the  $z$ -axis is more concentrated near the center ( $z = 0$ ) than the other two directions. As also characterized by the miscibility parameter,  $\eta = 0.77$ , in the present case the coupled system is partially miscible. This is quite well represented in the left four panels given in figure 3.

For the coupled system  $^{164}\text{Dy}$ – $^{162}\text{Dy}$  we use two other different set of parameters in our analysis, showing the densities of the two coupled components in 3D and 1D plots in the panels (e)–(h) of figures 2 and 3, respectively. These results are given in correspondence with the results presented for the system  $^{168}\text{Er}$ – $^{164}\text{Dy}$  in the panels (a)–(d) of figures 2 and 3. For the parameters, we have  $d_{11} = 31.42$ ,  $d_{12} = 1.040$ ,  $d_{22} = 1.065$  and  $d_{21} = 31.190$ , with  $N_1 = 1500$  and  $N_2 = 50$ , in the frames (e), (f) of figures 2 and 3; with  $d_{11} = 28.2$ ,  $d_{12} = 1.040$ ,  $d_{22} = 1.065$  and  $d_{21} = 28.071$ , with  $N_1 = 1350$  and  $N_2 = 50$ , in the frames (g), (h) of these figures. In this case, where we have two isotopes of the same atom, we notice that the system is completely miscible, having the same value close to one for the miscibility parameter  $\eta = 0.99$ . The complete overlap between the densities of the two components are clearly shown in panels (e)–(h) of figure 3.

In these figures 2 and 3, by using the aspect ratio  $\lambda = 7$ , for each one of the mixtures we can identify a non-trivial structure emerging in the condensate near the boundary of stability, with a local minimum at the center (for both components) in the symmetrical  $x$ – $y$  plane (see left panels of both figures). At the  $z$ -direction, we have a normal Gaussian shape, as seen in the right panels of the figures.

In both the mixtures shown in figures 2 and 3, the upper panels (a), (b) and (e), (f) are for parameters very close to the stability threshold, as indicated by the results given in figure 1. Therefore, the structure observed for the density of the component 1, which has the largest fraction of atoms in the coupled system, can be explained by fluctuations close to the instability regime. For each system, by going from smaller values, shown in panels (c), (d) and (g), (h), to larger values, shown in panels (a), (b) and (e), (f), of  $N_1$  (keeping  $N_2$  about the same), we are approaching the unstable regime, visualized by the occurrence of oscillation peaks in the density of the dominant component in the system. The observed number of four peaks around the center is related to stability requirements when the number of atoms is close to the maximum allowed limit for a given trap asymmetry. By small variations of the parameters near the stability, before the collapse of the system, it is possible to increase such number of peaks.

In both sets of systems shown in figures 2 and 3, while observing the peak oscillations occurring for the first component, one can observe only the biconcave-shaped condensate for the second component. In this regard, we should also note that biconcave-shaped structures with local minimum in dipolar BECs have already been reported in the cases of single component condensates. In [33], such structures are explained as due to roton instability for certain specific pancake-type trap aspect ratios  $\lambda$  ( $\approx 7, 11, 15, 19, \dots$ ), being not observed for other values of  $\lambda$ . In our analysis, we confirm the values reported in [33]. However, when considering single-component BECs, we have also verified these type of structures for other particular trap-aspect ratios, such as  $\lambda \approx 8, 12, 16$ , and 20. However, for the cases of fully anisotropic traps, where two aspect ratios are considered, this kind of density fluctuation has also been observed in [39], for single component dipolar BECs. When considering two-component systems, we have verified this kind of structured states with no particular restriction on the values of  $\lambda$ .



The biconcave structure occurs for particular aspect ratios of the trap, due to the repulsive interaction between the dipoles. In the present study for a coupled dipolar system, we observe that we have also the repulsive inter-species DDI in addition to the intra-species DDI, leading to the observed four peaks in the density oscillations. The biconcave structures with a local minimum and few peaks are occurring near unstable regimes, which makes the experimental reproduction non-trivial to be observed.

In order to illustrate the behavior of the coupled densities, as we go from the parameter region close to the border of stability to a more stable configuration, we show three illustrative density plots in figure 4 considering the particular case with  $\lambda = 8$  for the mixture  $^{168}\text{Er}-^{164}\text{Dy}$ , with fixed number of dysprosium atoms  $N_2 = 950$ . From the panels (a) to (c) we are varying the number of erbium atoms from 3000 to 2000. We notice that, by going from a more stable region (shown in panel (c), where  $N_1 = 2000$ ) to a region near the instability (panel (a), where  $N_1 = 3000$ ) the shape of the density distribution changes from a Gaussian to a biconcave format. By approaching very closely the instability region (increasing  $N_1$ ), one can observe the fluctuation in the density around the center.

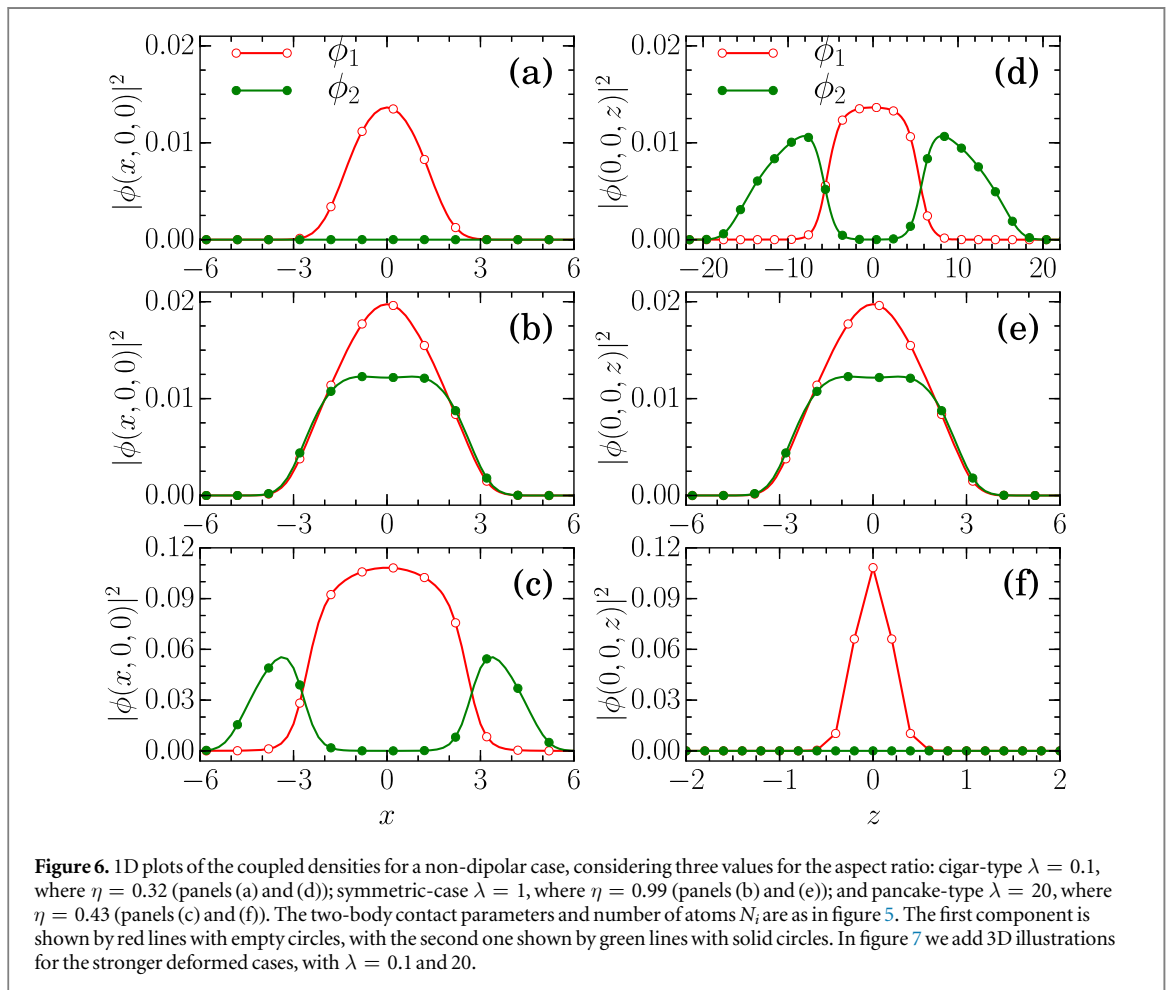
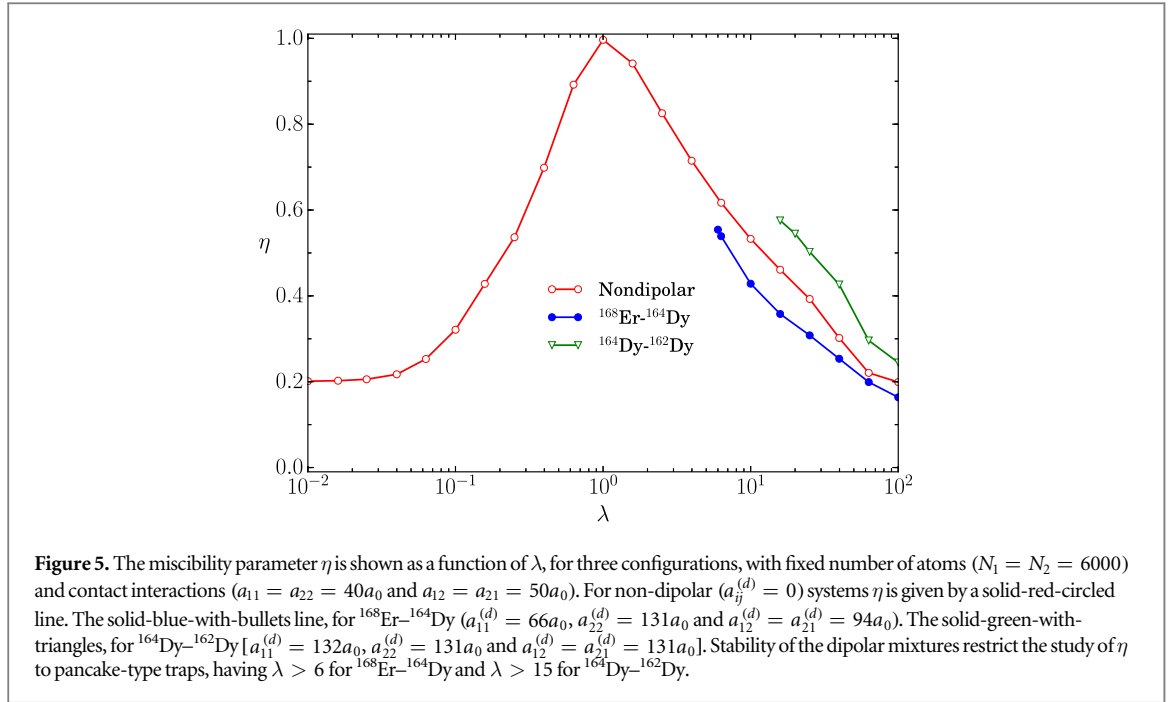
Besides the small mass difference between the atoms, in these cases of pure-dipolar coupled systems, the main difference is given by the respective dipolar interactions, which is directly related to the magnetic moment dipoles of the components. While for the  $^{168}\text{Er}-^{164}\text{Dy}$  we have quite different moment dipoles for the two atomic components (one is about half of the other), for the mixture  $^{164}\text{Dy}-^{162}\text{Dy}$  we have about the same dipolar parameters, with the inter- and intra-species interactions balancing each other. In view of that, the first mixture (with erbium) is expected to be more immiscible. This is reflected in the corresponding values of  $\eta$  ( $= 0.77$  for  $^{168}\text{Er}-^{164}\text{Dy}$ , and  $= 0.99$  for  $^{164}\text{Dy}-^{162}\text{Dy}$ ). The results for  $\eta$  are consistent with the approximate criterium that one could use for homogeneous mixtures, where we have  $\Delta \approx -0.014$  for  $^{168}\text{Er}-^{164}\text{Dy}$ , whereas  $\Delta \approx 0$  for  $^{164}\text{Dy}-^{162}\text{Dy}$ . However, with the parameter  $\eta$  we can have a more realistic indication of the partial overlap between the densities.

## 4.2. Miscibility in non-dipolar coupled systems

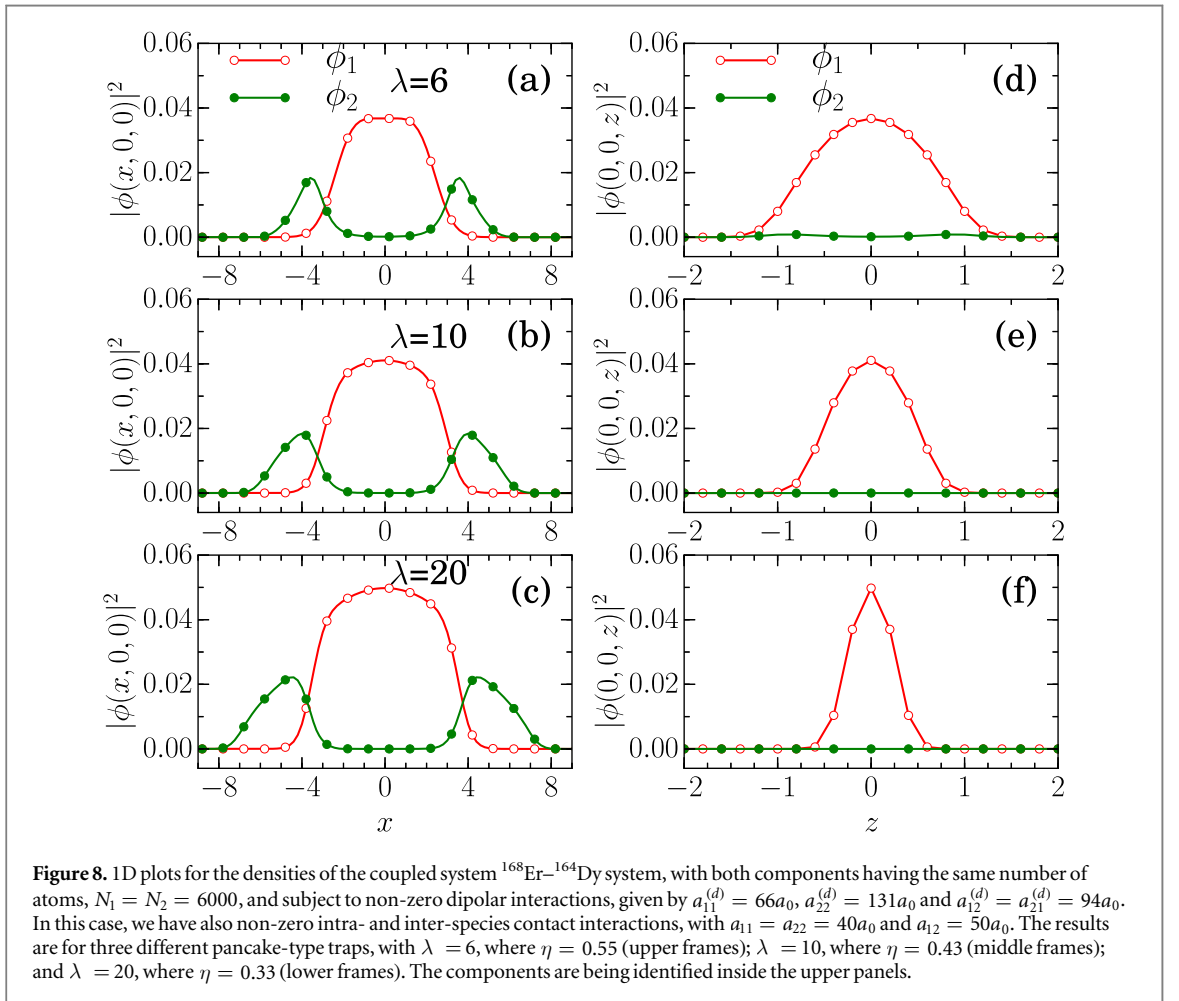
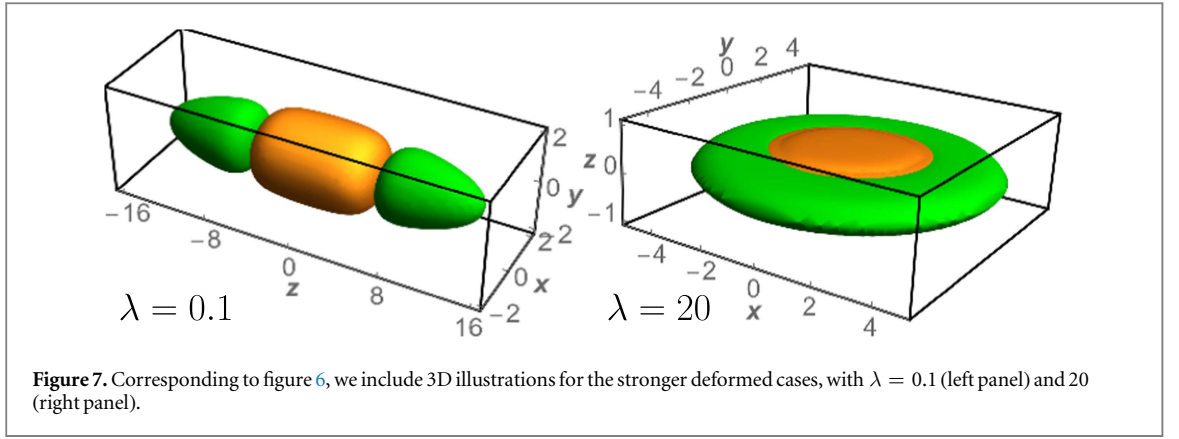
### 4.2.1. Role of the trapping aspect ratio

The effect of the geometry due to the external harmonic trap potential on the phase separation of the mixtures is investigated in the next, by considering different aspect ratios  $\lambda$  for the cases when the nonlinearity is given at least by repulsive two-body interactions. The miscibility parameter, given by the factor  $\eta$ , indicating the amount of mixing in the densities of the two-component, is presented as a function of  $\lambda$  in figure 5, for the case that two-body contact interactions are fixed such that  $a_{11} = a_{22} = 40a_0$  and  $a_{12} = 50a_0$ , with fixed number of atoms for both components. As discussed when this parameter was defined, a complete overlap between the densities implies in  $\eta = 1$ , being zero in the other limit of a complete immiscible system. For the given non-zero contact interactions, we observe that a complete miscible coupled dipolar system cannot be obtained within a stable configuration, as the maximum value verified for the miscibility parameter is below 0.6 for both dipolar systems and number of atoms that we have considered. However, as we have already pointed out in the previous subsection, a value of  $\eta$  near 1 is possible to be obtained in case of complete dipolar systems (when the contact interactions are set to zero).

The purpose of this subsection is mainly to discuss full non-dipolar systems, with results given in figure 5 for non-zero dipolar interactions (for the  $^{168}\text{Er}-^{164}\text{Dy}$ , as well as for  $^{164}\text{Dy}-^{162}\text{Dy}$ ). These two kind of mixtures are of interest to show how the dipolar interactions can modify the miscibility behavior of a coupled BEC system. As noticed by the red-solid line with empty circles given in this figure (with  $d_{ij} = 0$ ), for non-dipolar systems we can also obtain stable almost immiscible states in cigar-type configurations with  $\lambda < 1$ . With non-zero dipolar parameters, and considering the given contact interactions, stable condensates are limited to pancake-type



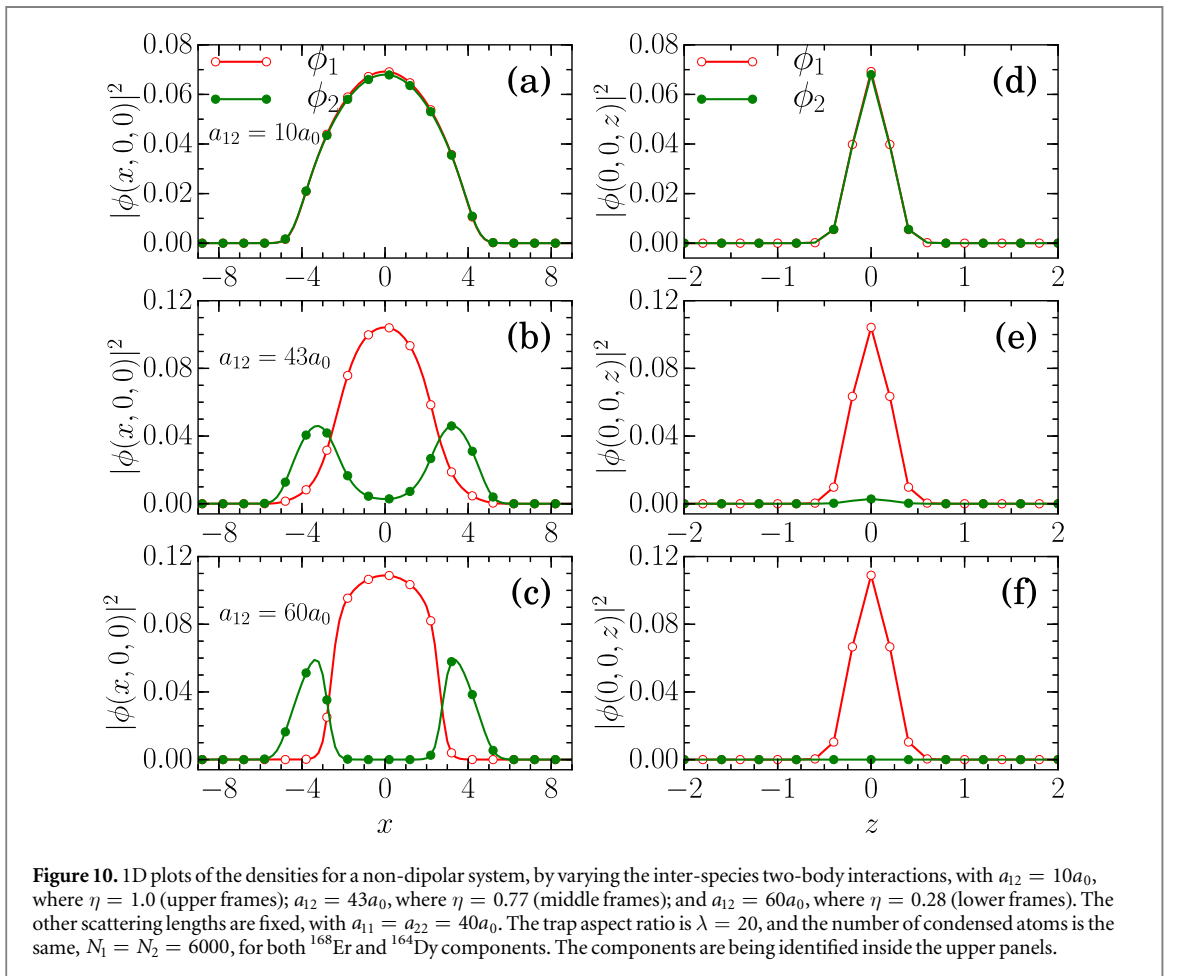
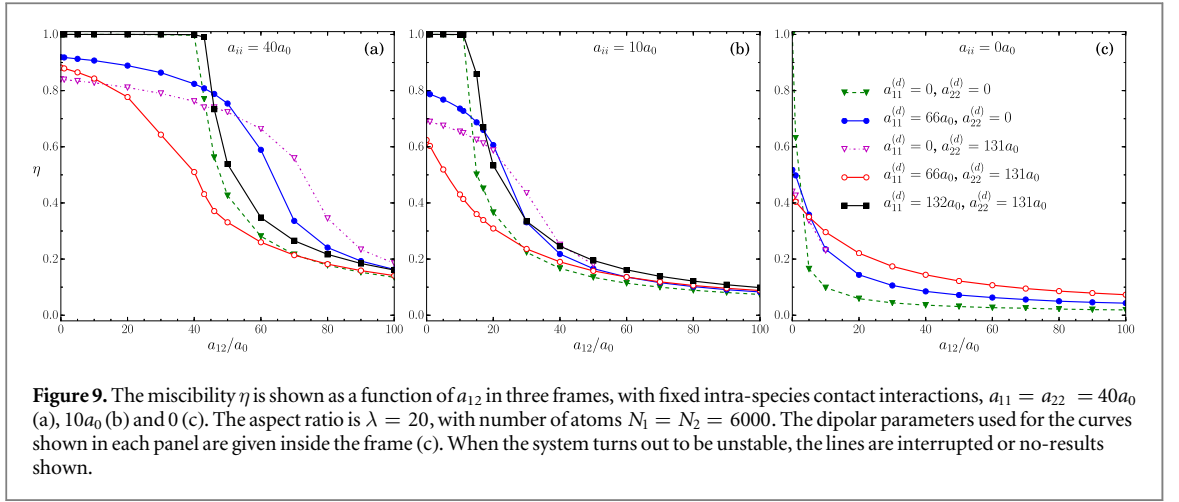
configurations with  $\lambda > 6$  for  $^{168}\text{Er}-^{164}\text{Dy}$  mixture; and  $\lambda > 15$  for the  $^{164}\text{Dy}-^{162}\text{Dy}$  mixture. As we can see from these results for a non-dipolar coupled system, the immiscibility is more evident when the trap is strongly deformed. It can happen for pancake-type traps, as well as for cigar-type traps. However, due to the stability of the condensates, it should be more favorable to build immiscible coupled condensates with pancake-type traps.



#### 4.2.2. Miscibility in cigar- and pancake-type traps

For non-dipolar mixtures, we resume our analysis by the 1D density plots given in figure 6, followed by a corresponding 3D illustration in figure 7. For the parameters we have both components with the same number of atoms ( $N_1 = N_2 = 6000$ ), and with repulsive two-body interactions such that  $a_{11} = a_{22} = 40a_0$  and  $a_{12} = 50a_0$ . In figure 6, the panels (a)–(c) display the central densities ( $y = z = 0$ ) as functions of  $x$ ; with the panels (d)–(f) showing the densities (for  $x = y = 0$ ) as functions of  $z$ .

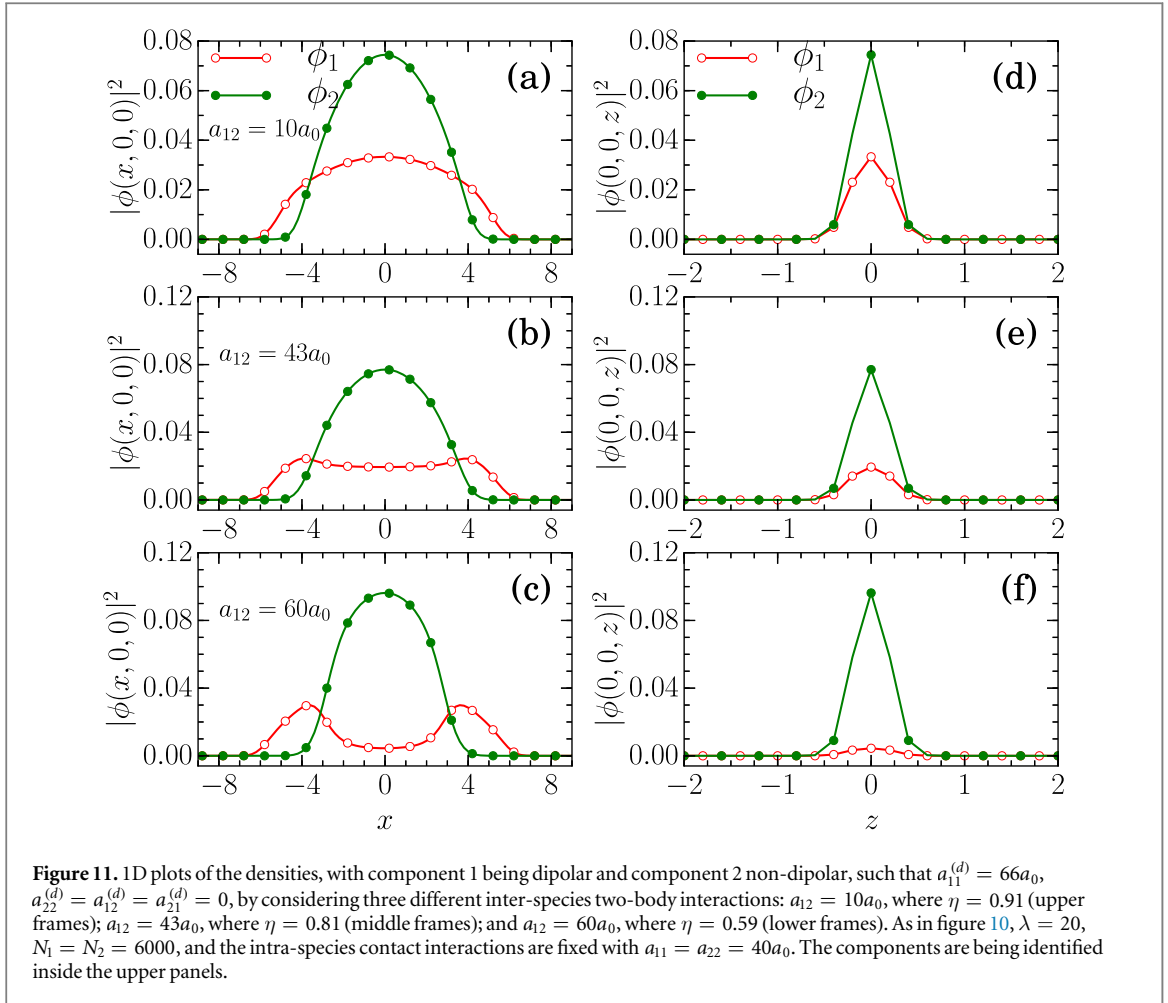
From these density plots, we can also infer how well the miscibility parameter  $\eta$ , given by (10), can be quantitatively used to estimate the miscibility condition of a two-component condensate. In the upper panels, (a) and (d), for a cigar-type trap with  $\lambda = 0.1$ , we have  $\eta = 0.32$ , which is quite well characterizing a situation when the component densities have their maximum at distinct positions, with a small overlap between them. Correspondingly, we observe similar relations between the value of  $\eta = 0.43$  and the distinct positions of the



extremes for the two components, in the case of a pancake-type trap with  $\lambda = 20$ , shown in panels (c) and (f). On the other hand, for  $\lambda = 1$ , shown in the panels (b) and (e), we can observe a strong superposition of the two components, with their maxima at the same position, with the miscibility parameter close to one ( $\eta = 0.99$ ).

The two 3D illustrations shown in figure 7, for the strong deformed cases with  $\lambda = 0.1$  (cigar type) and  $\lambda = 20$  (pancake type) are also characterizing the corresponding density distributions.

By considering the above discussion on the usefulness of the miscibility parameter  $\eta$ , in the next density results that will be shown we rely on the value of this parameter as a relevant quantitative observable for the miscibility analysis and corresponding surface visualization of the densities. As observed, for that we can take  $\eta < 0.5$  as being almost immiscible, with maxima for the two components in well distinct positions. In the other



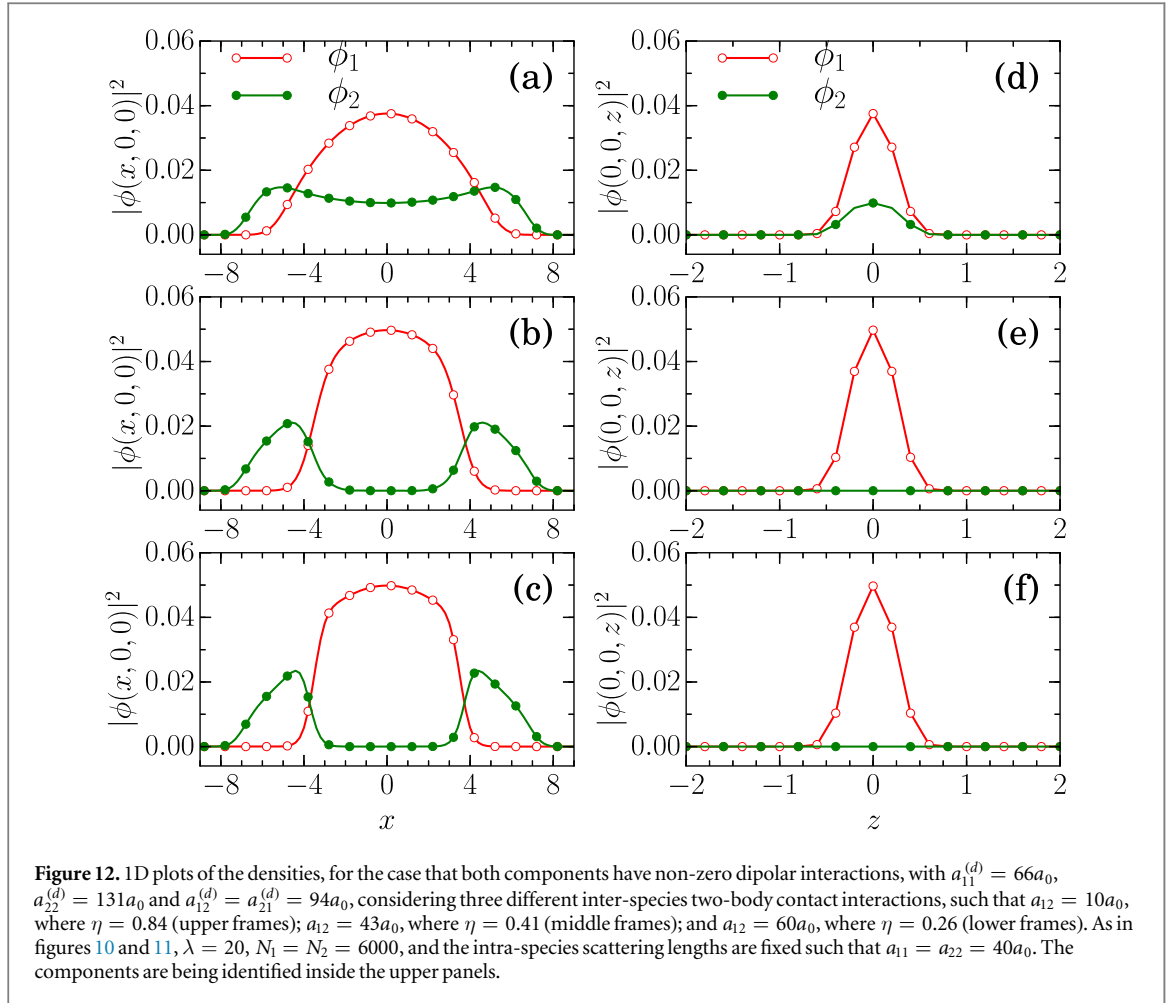
extreme, the system can be considered as almost miscible for  $\eta > 0.7$ . The other intermediate cases can be taken as partially miscible systems.

### 4.3. Miscibility in coupled BEC with dipolar and contact interactions

The miscibility behavior of the coupled condensate in terms of the aspect ratio  $\lambda$  is further investigated in figure 8 for dipolar systems in addition to the repulsive two-body contact interactions already used in figures 6, 7 ( $a_{11} = a_{22} = 40a_0$ ,  $a_{12} = 50a_0$ ). In this case, we consider the coupled system  $^{168}\text{Er}$ – $^{164}\text{Dy}$ , with the dipolar parameters given by  $a_{11}^{(d)} = 66a_0$ ,  $a_{22}^{(d)} = 131a_0$  and  $a_{12}^{(d)} = a_{21}^{(d)} = 94a_0$  (respectively, corresponding to  $d_{11} = 62.8$ ,  $d_{22} = 127.8$ ,  $d_{12} = d_{21} = 89.5$ ). By considering the same atom number for the components  $N_1 = N_2 = 6000$ , as verified before, stable results are possible only for pancake-type trapping potentials with  $\lambda > 6$ . In general, pancake traps provide strong axial confinement and help to increase the repulsive interaction along radial directions which guides to phase separation between the mixtures. In figure 8, by increasing the values for the aspect ratio (such as  $\lambda = 6, 10$  and  $20$ ), we can verify how the structure of the densities for the two components varies in an immiscible condition. The above observations for dipolar and non-dipolar BECs explain their specific characteristics. In particular, for erbium–dysprosium coupled dipolar condensate in stable configurations ( $\lambda > 6$ ), we are clarifying that it presents immiscible density structures, which are more pronounced for larger values of the trap-aspect ratio.

## 5. Miscibility results—role of the inter-species interaction

Besides the trap symmetry, another quite relevant parameter for the miscibility of coupled condensates is given by the inter-species interaction. In this case, when considering a system with fixed dipolarity, the appropriate parameter, which can be tuned via Feshbach resonance techniques [5], is given by the inter-species contact interaction. Therefore, our aim in the following analysis is to characterize the role of the inter-species scattering length  $a_{12}$  for the miscibility. For that, we assume both species have the same intra-species scattering lengths,  $a_{11} = a_{22} = 40a_0$ , choosing a particular large pancake-type trap with  $\lambda = 20$  and fixed number of atoms for

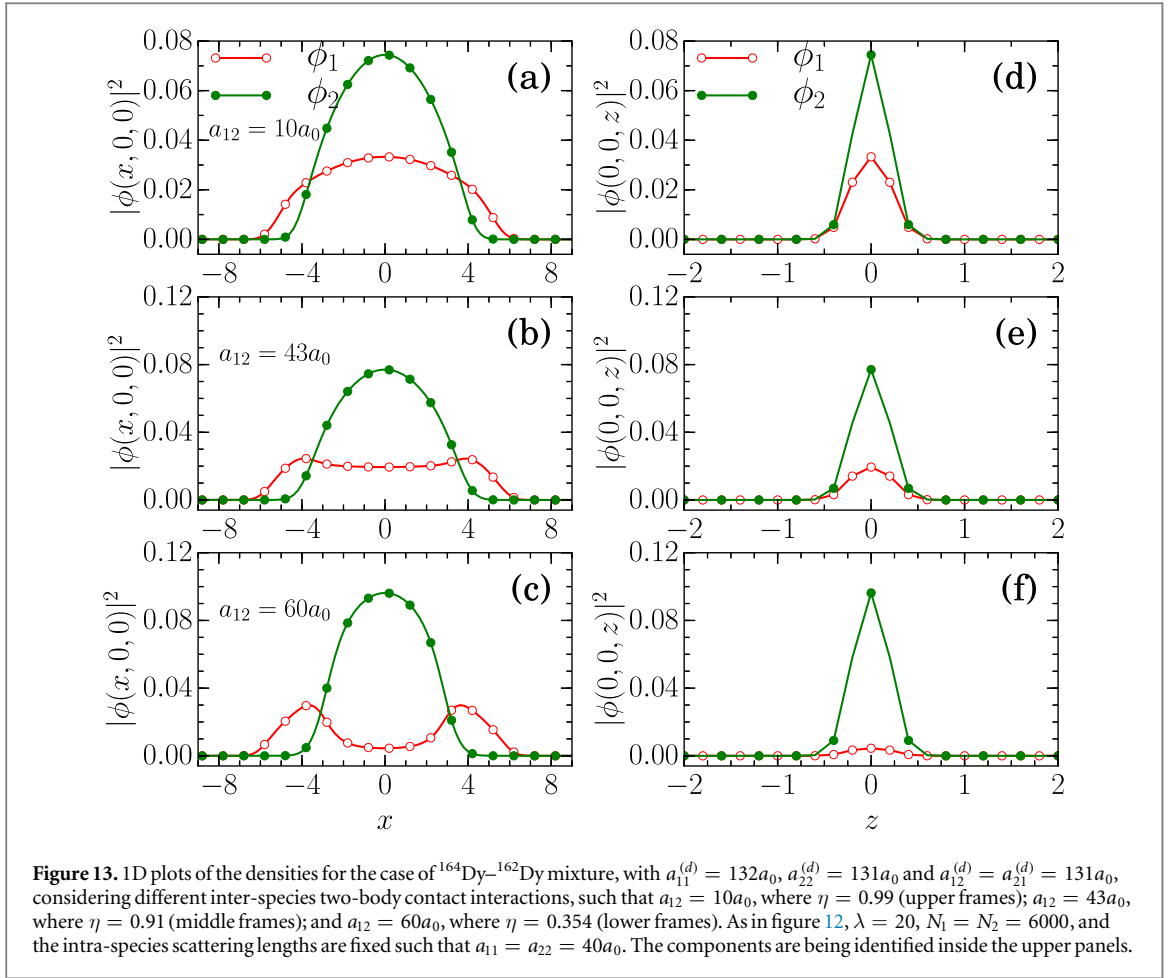


both components,  $N_1 = N_2 = 6000$ . These parameters are dictated by the previous stability analysis, looking for stronger characterization of miscibility properties.

The general behavior for the miscibility can be verified by the parameter  $\eta$ , which is shown in figure 9 as a function of the ratio  $a_{12}/a_0$ , considering three panels with different values for  $a_{ii}/a_0 = 40, 10$  and  $0$ . The parameter  $\eta$ , for the overlap between the two-component densities, is represented by considering five cases as indicated inside the frames, where in the frame (c) we have the dipolar parameters valid for the three frames. When both components are dipolar, the mixture  $^{168}\text{Er}-^{164}\text{Dy}$  is represented by the red curves with empty circles, with the mixture  $^{164}\text{Dy}-^{162}\text{Dy}$  represented by black curves with solid squares. When both components are non-dipolar, we show with green-curves with triangles. When only a single component has dipolar interactions, we have two cases, represented with blue curves with filled circles ( $a_{11}^{(d)} = 66a_0$ ,  $a_{22}^{(d)} = 0$ ) and magenta line with empty triangles ( $a_{11}^{(d)} = 131a_0$ ,  $a_{11}^{(d)} = 0$ ).

We should point out that the miscibility is going down slowly (increasing the immiscibility of the mixture) to an approximate constant value for  $a_{12} \rightarrow \infty$ . Even in the non-dipolar case: with  $a_{ii} = 40, 10$  and  $0$ , we have  $\eta \sim 0.14, 0.10$  and  $0.04$ , respectively. This can be understood from the residual mixing of the two-component wave-functions near the unitary limit of the inter-species (when  $a_{12} \rightarrow \infty$ ). In this limit for the inter-species, we should notice that we have the well-known Efimov effect [54], with increasing number of three-body bound and resonant states mixing the two component system. Already observed in cold-atom laboratories [55], this a pure quantum effect that occurs near zero two-body binding, when the effective potential goes as the inverse-square of the distance, and we have a long extension of the corresponding two-body wave functions. The role of this effect on coupled systems deserves further analysis in experiments, in particular when varying the mass-ratio of the mixture, as the resonant states have well-known theoretical predictions [56] also for mass-asymmetric mixtures.

Next, we can examine the role of the magnetic dipolar interactions in the miscibility of the two components. First, we should remind that these interactions between the magnetic dipoles are long-range ones, which go as the third power of the distance between the dipoles. They should act more effectively when the components are close together, but have residual effects due to long range behavior, which makes the miscibility be reduced to a non-zero constant value for  $a_{12} \rightarrow \infty$ , in a way similar to the non-dipolar case in this limit, such that we have



combined effects of two long-range interactions. In the other extreme, we can see the role of dipolar interactions in the miscibility by looking the region where  $a_{12} = 0$  in the panel (c). When we have no inter-species dipolar interactions (with only one of the species having magnetic moment) there is no coupling between the systems, such that the overlap between the densities is partial. One of the densities is given by a linear trapped equation; with the other given by a nonlinear equation (confined by the same harmonic trap, but additionally having the repulsive dipolar interaction). As larger is the effect due to repulsive dipolar interactions, less miscible is the system. When both intra-species dipolar interaction are switched on, we have also the corresponding inter-species parameter coupling the system, with the net repulsive effect being averaged out.

Another aspect verified in the panels of figure 9 refers to the stability of the system, which can be observed for this specific case that we have a pancake-shaped trap with  $\lambda = 20$  and fixed number of atoms  $N_i = 6000$ . When we have single dipolar interaction with larger strength as  $a_{22}^{(d)} = 131a_0$ , the stability can happen only for some limited values of the contact interactions, as indicated in the three panels by the maximum values obtained for  $a_{12}$ : for  $a_{ii} = 0$ , panel (c),  $a_{12} \leq 10a_0$ ; for  $a_{ii} = 10a_0$ , panel (b),  $a_{12} \leq 50a_0$ ; and with no limit in  $a_{12}$  when  $a_{ii} = 40a_0$ , as shown in panel (c). These upper limits in  $a_{12}$  for the stability result from the specific trap conditions and number of atoms we are considering, as one could trace, approximately, from the stability results shown in figure 1. Therefore, by reducing the number of atoms for the component 2, we could increase the upper limits for  $a_{12}$ .

In general, from figure 9 one can observe that the immiscibility will significantly increase by increasing  $a_{12}$  in all the verified situations. Also, by taking a fixed value for this inter-species contact interaction with  $a_{12} > a_{ii}$ , from the three panels one can verify that by decreasing the intra-species contact interactions  $a_{11} = a_{22}$ , the immiscibility of the system increases ( $\eta$  decreases).

Density profiles of the coupled system are represented in the next figures 10–13, where we show results considering three values of the two-body inter-species scattering lengths, with the corresponding intra-species contact interactions  $a_{ii}$  kept fixed at  $40a_0$ . In all these cases, in order to facilitate the comparison of the results, we assume the same three values for  $a_{12}$  ( $=10a_0$ ,  $43a_0$  and  $60a_0$ ) and maintain the trap-aspect ratio fixed to a pancake-type,  $\lambda = 20$ , with the number of particles given by  $N_1 = N_2 = 6000$ , as in the plotted results of figure 9. For a better quantitative comparison of the results, we present the densities in 1D plots, as functions of  $x$

(left panels) and  $z$  (right panels). In figure 10, we have the case of non-dipolar systems; in figure 11 when considering just one of the components being dipolar. In figures 12 and 13, we consider two cases, when both components are dipolar, with parameters corresponding to the mixtures  $^{168}\text{Er}-^{164}\text{Dy}$  and  $^{164}\text{Dy}-^{162}\text{Dy}$ , respectively.

First, by considering non-dipolar BECs, in figure 10, with three values for the inter-species scattering length, ( $a_{12}$  varying between 10 and  $60a_0$ , with  $a_{11} = a_{22} = 40a_0$ ). The transition is expected to occur close to  $a_{12} \approx a_{11}$  ( $m_1 \approx m_2$ ). This is consistent with the results shown in this figure, where we can verify that for  $a_{12} > a_{11}$  there is already a clear separation between the two species, with  $\eta = 0.28$  for  $a_{12} = 60a_0$ . It is also shown that for  $a_{12} = 10a_0$  the mixture is completely miscible ( $\eta = 1$ ), having a sudden transition for  $a_{12} = 43a_0$  (just above  $a_{11} = 40a_0$ ) to a partial immiscible state. By further increasing  $a_{12}$ , an almost complete immiscible state is reached (for  $a_{12} = 60a_0$ ,  $\eta = 0.28$ ).

Next, in figure 11, we study the case where only the component 1 is dipolar. By comparing with the non-dipolar case, we can observe the effect of the dipolar interaction in breaking the sudden transition verified when increasing the inter-species contact interaction, such that the transition is much softer than the one shown for the non-dipolar case.

In order to observe the effect in the miscibility when changing the inter-species scattering length for the cases that both components are dipolar, we present 1D plots for the densities in figures 12 and 13. For the kind of mixture considered in 12, the  $^{168}\text{Er}-^{164}\text{Dy}$ , we notice that the system is partially miscible even at  $a_{12} < a_{11}$ , becoming almost immiscible for  $a_{12} > 30a_0$ . However, in case of  $^{164}\text{Dy}-^{162}\text{Dy}$  mixture, we observe that the system is almost miscible for small inter-species scattering lengths, becoming immiscible as we increase the inter-species scattering length. Therefore, we clearly noticed from these two figures, the immiscibility increasing when the inter-species scattering length become dominant in respect to the dipolar interactions.

## 6. Summary and conclusion

Motivated by recent experimental studies with dipolar systems, we focus our study in the two coupled mixtures given by  $^{168}\text{Er}-^{164}\text{Dy}$  and  $^{164}\text{Dy}-^{162}\text{Dy}$ . In the present work, our approach was to evidence the miscibility properties of a coupled condensate with two different species of atoms, having contact or dipolar pairwise interaction between them. First, we did an investigation related to the stability of dipolar coupled systems, as one varies the trap-aspect ratio and the number of atoms of both species. For realistic number of atoms in a mixed BEC system, we found necessary to consider pancake-type configurations ( $\lambda > 1$ ) for the coupled condensates, when the dominant nonlinear interaction is dipolar. In order to be more complete on the characterization of miscibility, we have extended our study to non-dipolar systems in cigar-type configurations, where it was possible to point out strong immiscibility for the coupled system.

For the study of miscibility, we extended an approach for the critical conditions of homogeneous coupled systems confined in hard-wall barriers. We observed that the critical MIT conditions remain unaffected by the dipolar interactions, once all the parameters of the previous definition are rescaled by incorporating the dipolar ones. In order to measure the miscibility of a more general confined coupled system, a relevant parameter  $\eta$  was defined in terms of the two-component densities. For a general system, this parameter is shown to be adequate to verify the miscibility of a coupled system than the usually simplified criterium obtained for homogeneous systems from energy consideration, where the kinetic energy is ignored.

By studying the miscibility for pure-dipolar coupled system (zero two-body contact interactions), we first compare the properties of the two mixtures given by  $^{168}\text{Er}-^{164}\text{Dy}$  and  $^{164}\text{Dy}-^{162}\text{Dy}$ . Besides the small mass difference between the atoms in both this two mixtures, one should notice that the main difference in their respective dipolar interactions  $a_{ij}^{(d)}$  is due to the differences in the magnetic moment dipole of erbium and dysprosium atoms. As verified, the two mixtures have quite different miscibility behavior, with  $^{164}\text{Dy}-^{162}\text{Dy}$  being completely miscible ( $\eta = 0.99$ ) and  $^{168}\text{Er}-^{164}\text{Dy}$  partially miscible ( $\eta = 0.77$ ), when we fix to the same values the other parameters (trap-aspect ratio and number of atoms). Such behavior is clearly due to the inter-species dipolar strength in comparison with the intra-species one. In this pure-dipolar case, we are also pointing out some non-trivial biconcave-shaped structures, with local minimum states for both components of the coupled system and with the emergence of density oscillations (manifested by a few peaks), when the system is near the stability border. This behavior is verified for both coupled mixtures that we have examined, with no direct relation with the miscibility of the species. Already reported in [39], this kind of nontrivial biconcave configuration has also been observed for single component dipolar systems, with the density fluctuations attributed to roton mode of the condensates. The role of the trap aspect ratio and inter-species contact interaction for the miscible-immiscible phase transition was studied for different configurations, from non-dipolar to pure dipolar systems.

The present results on the miscibility are expected to be quite relevant in studies with dipolar and non-dipolar coupled systems, in order to set parameters in experimental realizations. Within this perspective, when considering dipolar systems, we choose atomic mixtures with large repulsive dipolar strengths that are being investigated in BEC laboratories. In a possible straightforward extension of this work, we could alter the confining conditions of both condensates, with their center being separated by some distance, or by using different aspect ratios. As another perspective for future developments, we can mention studies of systems under rotations, where rich vortex structures will emerge, by following recent interest in the subject that can be traced from [57] and references therein.

## Acknowledgments

RKK acknowledges the financial support from FAPESP of Brazil (Contract number 2014/01668-8). The work of PM forms a part of Science & Engineering Research Board, Department of Science & Technology (India) sponsored research project (No. EMR/2014/000644) and FAPESP (Brazil). AG and LT thank CAPES, CNPq and FAPESP of Brazil for partial support.

## ORCID iDs

Paulsamy Muruganandam  <https://orcid.org/0000-0002-3246-3566>

Lauro Tomio  <https://orcid.org/0000-0002-2811-9797>

## References

- [1] Anderson M H, Ensher J R, Matthews M R, Wieman C E and Cornell E A 1995 *Science* **269** 198–201  
Davis K B, Mewes M-O, Andrews M R, van Druten N J, Durfee D S, Kurn D M and Ketterle W 1995 *Phys. Rev. Lett.* **75** 3969–73  
Bradley C C, Sackett C A, Tollett J J and Hulet R G 1995 *Phys. Rev. Lett.* **75** 1687
- [2] Anglin J R and Ketterle W 2002 *Nature* **416** 211–8  
Chu S 2002 *Nature* **416** 206–10  
Bloch I, Dalibard J and Zwerger W 2008 *Rev. Mod. Phys.* **80** 885
- [3] Proukakis N P, Snoke D W and Littlewood P B (ed) 2017 *Universal Themes of Bose–Einstein Condensation* (Cambridge: Cambridge University Press)
- [4] Bloch I, Dalibard J and Nascimbène S 2012 *Nat. Phys.* **8** 267–76
- [5] Chin C, Grimm R, Julienne P and Tiesinga E 2010 *Rev. Mod. Phys.* **82** 1225
- [6] Greiner M, Regal C A and Jin D S 2003 *Nature* **426** 537–40  
Bloch I 2005 *Nat. Phys.* **1** 23–30  
Spielman I B, Phillips W D and Porto J V 2007 *Phys. Rev. Lett.* **98** 080404  
Büchler H P, Demler E, Lukin M, Micheli A, Prokof'ev N, Pupillo G and Zoller P 2007 *Phys. Rev. Lett.* **98** 060404  
Jördens R, Strohmaier N, Günter K, Moritz H and Esslinger T 2008 *Nature* **455** 204–7  
Kraft S, Vogt F, Appel O, Riehle F and Sterr U 2009 *Phys. Rev. Lett.* **103** 130401  
Schauss P, Cheneau M, Endres M, Fukuhara T, Hild S, Omran A, Pohl T, Gross C, Kuhr S and Bloch I 2012 *Nature* **491** 87–91
- [7] Myatt C J, Burt E A, Ghrist R W, Cornell E A and Wieman C E 1997 *Phys. Rev. Lett.* **78** 586
- [8] Chui S and Ryzhov V 2004 *Phys. Rev. A* **69** 043607
- [9] Hall D S, Matthews M R, Ensher J R, Wieman C E and Cornell E A 1998 *Phys. Rev. Lett.* **81** 1539
- [10] Tojo S, Taguchi Y, Masuyama Y, Hayashi T, Saito H and Hirano T 2010 *Phys. Rev. A* **82** 033609
- [11] Papp S B, Pino J M and Wieman C E 2008 *Phys. Rev. Lett.* **101** 040402
- [12] Ferrari G, Inguscio M, Jastrzebski W, Modugno G, Roati G and Simoni A 2002 *Phys. Rev. Lett.* **89** 053202  
Thalhammer G, Barontini G, De Sarlo L, Catani J, Minardi F and Inguscio M 2008 *Phys. Rev. Lett.* **100** 210402  
McCarron D J, Cho H W, Jenkin D L, Köppinger M P and Cornish S L 2011 *Phys. Rev. A* **84** 011603
- [13] Miesner H J, Stamper-Kurn D M, Stenger J, Inouye S, Chikkatur A P and Ketterle W 1999 *Phys. Rev. Lett.* **82** 2228
- [14] Law C K, Pu H, Bigelow N P and Eberly J H 1997 *Phys. Rev. Lett.* **79** 3105
- [15] Ao P and Chui S T 1998 *Phys. Rev. A* **58** 4836
- [16] Barankov R A 2002 *Phys. Rev. A* **66** 013612  
Esry B D 1998 *Phys. Rev. A* **58** 3399(R)
- [17] Abdullaev F K, Gammal A, Salerno M and Tomio L 2008 *Phys. Rev. A* **77** 023615
- [18] Pasquiou B, Maréchal E, Bismut G, Pedri P, Vernac L, Gorceix O and Laborthe-Tolra B 2011 *Phys. Rev. Lett.* **106** 255303
- [19] Wilson R M, Ticknor C, Bohn J L and Timmermans E 2012 *Phys. Rev. A* **86** 033606
- [20] Wen L, Liu W M, Cai Y, Zhang J M and Hu J 2012 *Phys. Rev. A* **85** 043602
- [21] Pattinson R W, Billam T P, Gardiner S A, McCarron D J, Cho H W, Cornish S L, Parker N G and Proukakis N P 2013 *Phys. Rev. A* **87** 013625  
Pattinson R W 2014 Two-component Bose–Einstein condensates: equilibria and dynamics at zero temperature and beyond *PhD Thesis* Newcastle University, Newcastle, UK
- [22] Polo J, Ahufinger V, Mason P, Sridhar S, Billam T P and Gardiner S A 2015 *Phys. Rev. A* **91** 053626
- [23] Liu I-K, Pattinson R W, Billam T P, Gardiner S A, Cornish S L, Huang T-M, Lin W-W, Gou S-C, Parker N G and Proukakis N P 2016 *Phys. Rev. A* **93** 023628
- [24] Balaž A and Nicolin A I 2012 *Phys. Rev. A* **85** 023613
- [25] Filatrella G, Malomed B A and Salerno M 2014 *Phys. Rev. A* **90** 043629

- [26] Sartori A, Marino J, Stringari S and Recati A 2015 *New J. Phys.* **17** 093036
- [27] Yi S and You L 2000 *Phys. Rev. A* **61** 041604(R)
- [28] Santos L, Shlyapnikov G V, Zoller P and Lewenstein M 2000 *Phys. Rev. Lett.* **85** 1791  
Santos L, Shlyapnikov G V, Zoller P and Lewenstein M 2000 *Phys. Rev. Lett.* **88** 139904 (erratum)
- [29] Góral K and Santos L 2002 *Phys. Rev. A* **66** 023613
- [30] Giovanazzi S, Görlitz A and Pfau T 2002 *Phys. Rev. Lett.* **89** 130401  
O'Dell D H J, Giovanazzi S and Eberlein C 2004 *Phys. Rev. Lett.* **92** 250401
- [31] Merhasin I M, Malomed B A and Driben R 2005 *J. Phys. B: At. Mol. Opt. Phys.* **38** 877–92
- [32] Bortolotti D C E, Ronen S, Bohn J L and Blume D 2006 *Phys. Rev. Lett.* **97** 160402
- [33] Ronen S, Bortolotti D C E and Bohn J L 2007 *Phys. Rev. Lett.* **98** 030406
- [34] Koch T, Lahaye T, Fröhlich B, Griesmaier A and Pfau T 2008 *Nat. Phys.* **4** 218–22
- [35] Lahaye T, Metz J, Fröhlich B, Koch T, Meister M, Griesmaier A, Pfau T, Saito S, Kawaguchi Y and Ueda M 2008 *Phys. Rev. Lett.* **101** 080401
- [36] Wilson R M, Ronen S, Bohn J L and Pu H 2008 *Phys. Rev. Lett.* **100** 245302
- [37] Gligorić G, Maluckov A, Stepić M, Hadžievski L and Malomed B 2010 *Phys. Rev. A* **82** 033624
- [38] Asad-uz-Zaman M and Blume D 2011 *Phys. Rev. A* **83** 033616
- [39] Martin A D and Blakie P B 2012 *Phys. Rev. A* **86** 053623
- [40] Young S L E and Adhikari S K 2012 *Phys. Rev. A* **86** 063611  
Young S L E and Adhikari S K 2013 *Phys. Rev. A* **87** 013618
- [41] Bisset R N and Blakie P B 2013 *Phys. Rev. Lett.* **110** 265302  
Bisset R 2013 Theoretical study of the trapped dipolar Bose gas in the ultra-cold regime *PhD Thesis* University of Otago, Dunedin, New Zealand
- [42] Aikawa K, Frisch A, Mark M, Baier S, Rietzler A, Grimm R and Ferlaino F 2012 *Phys. Rev. Lett.* **108** 210401  
Frisch A 2014 Dipolar quantum gases of erbium *PhD Dissertation* University of Innsbruck, Innsbruck
- [43] Baranov M A 2008 *Phys. Rep.* **464** 71–111
- [44] Lahaye T, Menotti C, Santos L, Lewenstein M and Pfau T 2009 *Rep. Prog. Phys.* **72** 126401
- [45] Ueda M 2010 *Fundamentals and New Frontiers of Bose–Einstein Condensation* (Singapore: World Scientific Publ. Co.)
- [46] Griesmaier A, Werner J, Hensler S, Stuhler J and Pfau T 2005 *Phys. Rev. Lett.* **94** 160401  
Lahaye T, Koch T, Fröhlich B, Fattori M, Metz J, Griesmaier A, Giovanazzi S and Pfau T 2007 *Nature* **448** 672–5
- [47] Ni K-K, Ospelkaus S, Wang D, Quémener G, Neyenhuis B, de Miranda M H G, Bohn J L, Ye J and Jin D S 2010 *Nature* **464** 1324–8
- [48] Lu M, Youn S H and Lev B L 2010 *Phys. Rev. Lett.* **104** 063001  
Lu M, Burdick N Q, Youn S H and Lev B L 2011 *Phys. Rev. Lett.* **107** 190401  
Tang Y, Burdick N Q, Baumann K and Lev B L 2015 *New J. Phys.* **17** 045006
- [49] Ferrier-Barbut I, Kadau H, Schmitt M, Wenzel M and Pfau T 2016 *Phys. Rev. Lett.* **116** 215301
- [50] Inouye S, Andrews M R, Stenger J, Miesner H J, Stamper-Kurn D M and Ketterle W 1998 *Nature* **392** 151–4  
Hussein M S, Timmermans E, Tommasini P and Kerman A K 1999 *Phys. Rep.* **315** 199–230
- [51] Gammal A, Frederico T and Tomio L 2001 *Phys. Rev. A* **64** 055602  
Gammal A, Tomio L and Frederico T 2002 *Phys. Rev. A* **66** 043619  
Brтка M, Gammal A and Tomio L 2006 *Phys. Lett. A* **359** 339
- [52] Kumar R K, Young S L E, Vudragović D, Balaž A, Muruganandam P and Adhikari S K 2015 *Comput. Phys. Commun.* **195** 117–28
- [53] Lončar V, Balaž A, Bogojević A, Škrbić S, Muruganandam P and Adhikari S K 2016 *Comput. Phys. Commun.* **200** 406–10  
Satarić B, Slavnić V, Belić A, Balaž A, Muruganandam P and Adhikari S K 2016 *Comput. Phys. Commun.* **200** 411  
Lončar V, Young S L E, Škrbić S, Muruganandam P, Adhikari S K and Balaž A 2016 *Comput. Phys. Commun.* **209** 190
- [54] Efimov V 1970 *Phys. Lett. B* **33** 563–4  
Efimov V 2009 *Nat. Phys.* **5** 533–4
- [55] Kraemer T et al 2006 *Nature* **440** 315–8  
Ferlaino F and Grimm R 2010 *Physics* **3** 1–21
- [56] Frederico T, Tomio L, Delfino A and Amorim A E A 1999 *Phys. Rev. A* **60** R9–12  
Braaten E and Hammer H-W 2006 *Phys. Rep.* **428** 259–390
- [57] Kumar R K, Sriraman T, Fabrelli H, Muruganandam P and Gammal A 2016 *J. Phys. B: At. Mol. Opt. Phys.* **49** 155301